A Hierarchical Architecture for Cooperative Actuator Fault Estimation and Accommodation of Formation Flying Satellites in Deep Space

S.M. Azizi and K. Khorasani

***Abstract*—In this paper, a new cooperative fault accommodation algorithm based on a multi-level hierarchical architecture is proposed for satellite formation flying missions. This framework introduces a high level (HL) supervisor and two recovery modules, namely a low level fault recovery (LLFR) module and a formation level fault recovery (FLFR) module. At the low level fault recovery (LLFR) module, a new hybrid and switching framework is proposed for cooperative actuator fault estimation of formation flying satellites in deep space. The formation states are distributed among local detection and estimation filters. Each system mode represents a certain cooperative estimation scheme and communication topology among local estimation filters. The mode transitions represent the reconfiguration of the estimation schemes, where the transitions are governed by information that is provided by the detection filters. It is shown that our proposed hybrid and switching framework confines the effects of unmodeled dynamics, disturbances, and uncertainties to local parameter estimators, thereby preventing the propagation of inaccurate information to other estimation filters. Moreover, at the low level fault recovery (LLFR) module a conventional recovery controller is implemented by using estimates of the fault severities. Due to an imprecise fault estimate and an ineffective recovery controller, the high level (HL) supervisor detects violation of the mission error specifications. The formation level fault recovery (FLFR) module is then activated to compensate for the performance degradations of the faulty satellite by requiring that the healthy satellites allocate additional resources to remedy the problem. Consequently, fault is cooperatively recovered by our proposed architecture, and the formation flying mission specifications are satisfied. Simulation results confirm the validity and effectiveness of our developed and proposed analytical work.**

***Index Terms*—Cooperative Estimation, Fault Accommodation, Formation Flight Satellites, Hierarchical Systems, Distributed Kalman Filter, Distributed Control, Fault Tolerant Control Systems, Reconfigurable Controllers**

LIST OF ACRONYMS

LL	Low level	MIMO	Multiple-input multiple-output
FL	Formation level	L/F	Leader/follower
HL	High level	VS	Virtual structure
LLFR	Low level fault recovery	EF	Estimation filter
FLFR	Formation level fault recovery	IMM	Interactive multiple model
FFC	Formation flying control	PHA	Probabilistic hybrid automata

S.M. Azizi and K. Khorasani are with the Electrical and Computer Engineering Department, Concordia University, Montreal, Quebec, H3G 1M8, Canada (e-mail: {seyye_az,kash}@ece.concordia.ca).

This research is supported in part by grants from the Discovery program and the Strategic Projects program of the Natural Sciences and Engineering Research Council of Canada (NSERC).

FDIR	Fault detection, isolation, and recovery	AFF	Autonomous formation flying
DS	Deep space	DES	Discrete-event system
CKF	Centralized Kalman filter	LTI	Linear time-invariant
RDKF	Reconfigurable distributed Kalman filter	LTV	Linear time-varying
DF	Detection filter		

I. Introduction

Formation flying is relatively a new concept envisaged for a cluster of satellites that calls for development of novel technologies. This new field has been surveyed in detail in [1] and [2], where five architectures are introduced for formation flying control (FFC), namely Multiple-Input Multiple-Output (MIMO), Leader/Follower (L/F), Virtual Structure (VS), Cyclic and Behavioral. Due to the high-precision control requirements, the problem of fault diagnosis, estimation, and recovery of formation flying missions has become particularly significant and crucial. Various methods have been developed and proposed in the literature for the problem of fault detection and isolation, fault estimation, and recovery in a single satellite. However, none of these works have formally investigated the concept of cooperative fault estimation and accommodation in formation flying satellites.

In this paper, the problem of fault estimation and accommodation in formation flying control (FFC) of satellites is investigated by using a *cooperative scheme*. This cooperative scheme was initially proposed by the authors in [3], [4], [5], [6] and is formulated in this paper for the general case of multiple-satellite formation. The cooperative formation diagnosis and control problem is constrained by the availability of only relative state measurements in deep space (DS), subject to unmodeled dynamics, uncertainties and disturbances (for instance, these can be manifested as undesirable and unexpected communication delays among the satellites). The objective of our cooperative scheme is to constrain the impacts of unmodeled dynamics and uncertainties (such as those due to communication delays) on the local fault estimates and prevent the propagation of undesirable errors into the entire formation. In case that a fault estimate is not accurate within an acceptable tolerance level, cooperative recovery controllers will be activated to account for the resulting performance degradations (as manifested in tracking errors) of the formation mission. In the following, relevant results on fault detection and isolation, fault estimation, fault accommodation and recovery problems are reviewed in order to properly motivate and position the contribution and novelty of our proposed approach.

The problems of fault detection and isolation, fault estimation and recovery have been extensively investigated in the literature. In [7], fault detection in satellites is performed based on a fault tree approach, through which the fault cause is identified. In [8], fault detection is achieved through correlated decision fusion, in which two correlation models are proposed to approximate the complicated correlation among sensor measurements for general systems. In [9] and [10], a multiple model adaptive estimation approach and a bank of interacting Kalman filters, respectively, are used to detect sensor and actuator faults. In [11], decentralized estimation algorithms are surveyed and applied to state estimation of formation flying satellites. In [12], state estimation is performed by using a parallel operation of full-order observers with local measurements. A necessary condition on the communication topology is obtained to guarantee stability of simultaneous parallel estimators and controllers. The work in [13] deals with reduced-order distributed Kalman filters to minimize the computational cost. The overall system model is partitioned into several subsystems according to the physical considerations of the system, and a local Kalman filter is designed for state estimation in each subsystem. The robust decentralized approach in [14] is based on sliding mode observers to detect and estimate actuator faults in large-scale systems. In [15], a statistical local approach is specifically designed for

diagnosis and identification of faults with very small magnitudes.

The reconfigurable fault-tolerant control system approaches are reviewed in [16]. In [17], a fault tolerant control system is designed in which the problem of performance degradation is explicitly considered. In [18], a reconfigurable control allocation technique is applied to accommodate the aircraft control effector failures. In [19], the problem of fault estimation and control reconfiguration is studied in detail based on dynamic models, observers, and Kalman filters. In [20], the problems of fault diagnosis and fault tolerant control are investigated for a class of nonlinear systems based on nonlinear observer techniques. In [21], a fault is assumed to belong to a finite set of parameters (modes), and a sliding mode controller is designed for accommodation of each mode in a hierarchical framework. In [22], by solving a Lyapunov equation a robust state-space observer is proposed to simultaneously estimate descriptor system states, actuator faults, their finite time derivatives, and attenuate input disturbances to any desired accuracy. Moreover, a fault-tolerant control scheme is developed by using the estimates of descriptor states and faults. In [23], an adaptive Kalman filtering algorithm is developed to estimate the reduction of the control effectiveness in a closed-loop setting. The state estimates are fed back to achieve steady-state regulation, while the control effectiveness estimate is used for an on-line tuning of the control law. In [24], in order to diagnose thruster faults in satellite systems, the authors designed an iterative learning observer, which uses a learning mechanism instead of employing integrators that are commonly used in classical adaptive observers. In [25], fault detection, isolation and recovery (FDIR) is performed for nonlinear satellite models by using the parameter estimation approach and adaptively redesigning and reconfiguring the controllers.

The above referenced estimation and accommodation approaches do not attempt to constrain the effects of unmodeled dynamics, uncertainties and disturbances through a cooperative fault estimation and accommodation methodology. Most of the above cited fault estimation approaches have also been applied to a single satellite and are not designed specifically for a formation flight of satellites. In this work, a hierarchical fault estimation and an accommodation architecture is proposed in which the cooperation among different levels and modules of the formation aims at constraining the effects of unmodeled dynamics, uncertainties and disturbances. Moreover, it is shown that in presence of unmodeled dynamics, uncertainties and disturbances, a centralized estimation scheme has major drawbacks that can be effectively and efficiently handled and tackled by using our proposed cooperative estimation technique.

II. General Framework

Our proposed framework for cooperative fault estimation and accommodation is shown in Figure 1. In this figure, the solid and dashed lines represent internal and inter-level information exchanges, respectively, that are of the main concern in this paper. The bus lines, which are indicated by thick (gray) bidirectional arrows, represent the general information exchanges among different modules of the formation. The general information exchanges include the necessary communication protocols whose analysis falls beyond the scope of this work and is left as a topic of future research. The communication protocols require specific handshaking, parity, and other types of signals that are communicated among different modules. The exchange of information among satellites is introduced for two main purposes, namely estimation and control. In the case of an estimation problem, each satellite communicates relevant actuator and sensor measurement signals with its neighbors, while in the case of a control problem, each satellite communicates merely its sensor measurement signals. Our proposed cooperative fault estimation and accommodation framework includes a low level fault recovery (LLFR) module, a formation level fault recovery (FLFR) module, and a high level (HL) supervisor, whose descriptions are briefly presented next.

The low-level fault recovery (LLFR) module first detects and determines the severity of actuator faults by using conventional Kalman filtering techniques based on a new hybrid and switching framework. The high-level (HL) “supervisor” then makes a

decision on reconfiguring the invoked fault estimation scheme. The goal of the HL supervisor, which is represented by a discrete-event system (DES) [27], is to achieve an optimal and efficient cooperation (in the sense of communication and exchange of information) among local detection and estimation filters in order to limit and constrain the impacts of unmodeled dynamics, uncertainties and disturbances on the local estimation filters and prevent the propagation of undesirable errors into the entire formation. Once an actuator fault is estimated at the low level, the LLFR module in effect implements the "controller reconfiguration" by incorporating the fault estimates in the LLFR controller to improve the overall mission performance by reducing the tracking errors. Subsequently, the HL supervisor evaluates the performance of the LL-recovered (faulty) satellite with respect to and in view of the overall mission specifications. In case that the faulty satellite is deemed to be "partially" LL-recovered, that is it violates the overall mission error specifications, the supervisor makes a decision regarding the "formation structure reconfiguration" by the formation-level fault recovery (FLFR) module. This module suggests and produces a new structure by invoking the cooperation of all the other satellites to fully accommodate the partially LL-recovered satellite due to its performance degradations. Consequently, the fault is cooperatively accommodated by the LLFR and FLFR modules. The above descriptions state the main principles behind our proposed cooperative fault estimation and accommodation scheme.

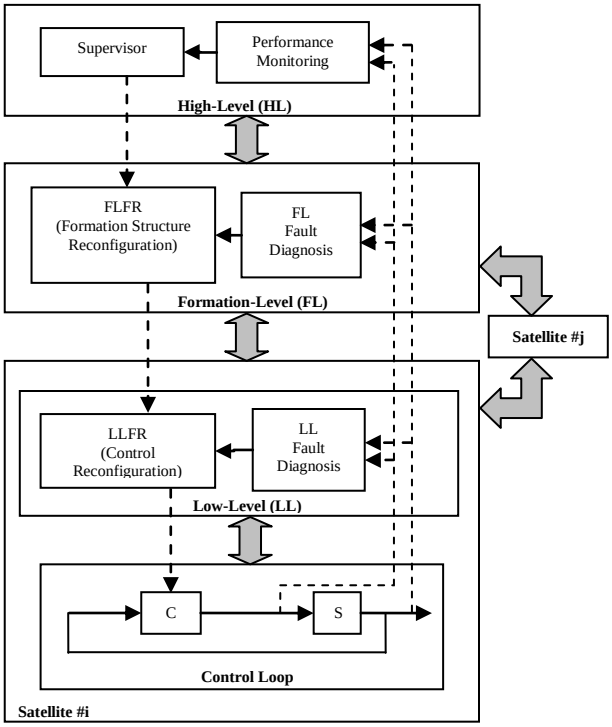

Figure 1. The proposed cooperative fault estimation and accommodation architecture.

In Figure 1, the LL module is located at the satellite level, and each satellite has its own LL fault diagnosis and LL fault recovery (LLFR) modules. The FL and HL modules include algorithms that necessitate the implementation of a central unit among the satellites. Therefore, these modules are located on a central satellite which has the most powerful communication resources and the best visibilities with respect to all the other satellites. However, redundant copies of the FL and HL algorithms can be uploaded onto other satellites as a backup for emergency circumstances when the communication resources of the central satellite degrades due to communication failures, or in circumstances when the visibility of the central satellite decreases due to the placement of other satellites in its blind spots.

In order to streamline, motivate and facilitate the transitions among the subsequent sections of this work, the following

observations are now stated, specifically:

(i) This paper considers only the position dynamics of the satellites in free space. Assuming that the thrusters are capable of generating any force in the three-dimensional space, the dynamics of satellites can be considered to be decoupled in the three axes of an inertial reference frame. This is a conventional technique that is used in the literature [28], e.g. as used in deriving the Hill's equation of motion in the planetary orbital environment (POE), in which the orbital dynamics of a satellite is considered to be independent of the attitude dynamics.

(ii) In this work, one of the sources of unmodeled dynamics, uncertainties and disturbances considered is due to the manifestations of undesirable and unexpected communication delays among the satellites. A communication delay can be induced intrinsically by the communication network or manifested due to the packet dropout in an imperfect communication channel [26].

(iii) The faults are augmented to the satellite states and will be considered as additional (fault) states. Estimation filters are used to estimate all the additional (fault) states, as it is not a standard approach to detect states by using detection filters. On the other hand, the detection filters are only used for the purpose of detecting the unmodeled dynamics and disturbances, which affect the dynamics of the satellite through an external input channel.

(iv) All the faults considered in this work occur in the satellite actuators and they are modeled by the corresponding fault parameters which are then augmented to the states of the system. The case of sensor faults can similarly be investigated, although not formally addressed in this paper and is left as a topic of future work. Furthermore, a sensor fault can be represented as an equivalent actuator fault provided that certain observability condition holds as described in [29]. In addition multiple actuator faults can be present which implies that multiple nonzero fault parameters can be estimated by the LLFR module. However, as far as the accommodation scheme is concerned it is assumed that only one satellite can be partially LL-recovered, and hence will need to be accommodated by the FLFR module. The problem of the FLFR for multiple partially LL-recovered satellites is left as a topic of future research.

(v) The HL supervisor is to be implemented and designed as a discrete-event system (DES) [27]. The details and procedures for these are not presented here as they are beyond the scope of this work. However, in order to demonstrate the "functionality" of a HL supervisor in this work, for the fault estimation scheme a hybrid and switching framework is presented that plays the role of a HL supervisor. By using information from the detection filters, the HL supervisor reconfigures the estimation filters to minimize the effects of unmodeled dynamics, uncertainties, and disturbances. Within the fault accommodation scheme, the HL supervisor is considered as a simple limit-checker, which takes into account the output measurements from all the sensors, compares them with the desired outputs, and determines whether the tracking errors are less than a certain error specification (e_s) associated with the overall formation mission. In other words, the HL supervisor (as a limit-checker) determines whether the mission specifications are satisfied or not.

(vi) In this work, we assume that there are no high-level faults in the formation mission. Specifically, we are only concerned with low-level faults (also known as component level faults) and among which we mainly focus on actuator faults. The high-level fault considerations are beyond the scope of this work. Fault diagnosis in discrete-event systems (DES) which can play the role of a HL supervisor is studied in [30].

(vii) In our envisaged switching estimation/control framework, the *dwell time* is defined as a positive time constant that guarantees stability of the system provided that the consecutive switching times among controllers and estimators are larger than the dwell time [31]. Analysis of the switching limitations of the dwell time is also beyond the scope of this paper, and therefore for sake of simplicity we assume that this condition is implicitly satisfied before any switching among estimators as well as control reconfigurations takes place.

(viii) The overall sequence of procedures that are invoked in this work can be briefly described as follows: In step 1, faults are cooperatively estimated by using the LL estimation filters. The HL supervisor decisions (through its hybrid and switching framework that aims at minimizing the effects of unmodeled dynamics, uncertainties, and disturbances) and the fault estimates are then incorporated into the LLFR controller. In step 2, the HL supervisor (as a limit-checker) determines whether the mission specifications are satisfied or not, and correspondingly activates the FLFR module if a satellite is partially LL-recovered. Finally in step 3, the FLFR module accommodates the partially LL-recovered satellite to preserve and maintain the overall formation mission.

III. Cooperative Fault Estimation by the LLFR Module

In this section, the notion of cooperative fault estimation is introduced and developed corresponding to the LLFR module to compensate for the effects of actuator faults. We consider an *N*-satellite formation in deep space, where the satellites orbital dynamics are approximated by double integrators [1], [2]. By invoking the observation **(i)** in Section II, we first express the absolute dynamics of a satellite in the local inertial frame that is defined by the *x*, *y* and *z* coordinates. However, due to the fact that an accurate absolute position measurement in deep space is not feasible, and due to the availability of relative position measurement sensors among the satellites in deep space, we will use the relative dynamics (that is, relative measurements among the satellites) for representing the orbital dynamics of the satellites in formation.

As stated above, given that the orbital dynamics of satellites are decoupled along the three *x*, *y* and *z* axes, we only consider the *x*-axis dynamics in this work as all the results can be similarly extended to the other two axes. The *x*-axis dynamics of the *i*-th satellite, $i = 1,\ldots,N$, including the external disturbances and sensor measurement noise are governed by

$$\begin{aligned} \dot{\theta}_{x_i}(t) &= \begin{bmatrix} 0 & 1 \\ 0 & 0 \end{bmatrix} \theta_{x_i}(t) + \begin{bmatrix} 0 \\ \dfrac{b_{x_i}}{m_i} \end{bmatrix} u_{x_i}(t) + \underbrace{\begin{bmatrix} 0 \\ d_x \end{bmatrix}}_{W_{x_i}} \\ z_{x_i}(t) &= \begin{bmatrix} 1 & 0 \end{bmatrix} \theta_{x_i}(t) + V_{x_i} \end{aligned} \tag{1}$$

where $\theta_{x_i} = (x_i, v_{x_i})^T \in R^2$, $u_{x_i} \in R$, and $z_{x_i} \in R$ denote the *x*-axis state vector (including the position x_i and the velocity v_{x_i}), the control input (actuator force), and the output (measured state) of the satellite #*i* ($i \in \{1,\ldots,N\}$), respectively, expressed in the local inertial frame. Moreover, the total mass of the satellite #*i* is denoted by m_i, and the external disturbances and the sensor measurement noise are represented by $W_{x_i} = [0 \quad d_x]^T$ (d_x is the corresponding scalar disturbance) and V_{x_i}, respectively. The subscript "x_i" used above (as in θ_{x_i} and z_{x_i}) represents the *x*-axis variables of the satellite #*i*. In addition,

$$b_{x_i} = \bar{b}_{x_i} + f_{x_i} \tag{2}$$

denotes the *x*-axis actuator gain, in which $\bar{b}_{x_i}$ and f_{x_i} represent the *x*-axis nominal (healthy) actuator gain and its corresponding loss-of-effectiveness fault signal, respectively. It should be pointed out that the faults considered in this work are of permanent nature and as stated earlier correspond only to actuators. It should be noted that a "permanent" fault is not necessarily constant and can be time-varying, as opposed to an "intermittent" fault which is present for usually irregular intervals of time. Due to the nature of an intermittent fault, it can be argued that an effective approach for modeling these faults is through an event-based framework, e.g. through a discrete-event system (DES) model [32], or a finite state machine, e.g. through Markov models [33], but this consideration is beyond the scope of this work.

In the normal (healthy) operational mode of a satellite, the fault parameter is considered to be zero (that is, $f_{x_i} = 0$). In the

faulty operational mode of a satellite, the case of a time-varying fault signal (that is, $\dot{f}_{x_i} \neq 0$ as a source of unmodeled dynamics and disturbance) has already been studied by the authors in [5] and is not the focus this paper. On the other hand, the main focus of this paper is on communication delays as a source of unmodeled dynamics and disturbances. Therefore, for the sake of simplicity in our analysis, let us assume that the fault signal is time-invariant or can be approximated as a slowly time-varying signal (that is, $\dot{f}_{x_i} = 0$). In order to estimate the severity of the fault, a conventional method for joint state-parameter estimation would be to augment the fault variable f_{x_i} to the state vector θ_{x_i} in order to form an overall extended system, which now becomes a more complex bilinear system [34] (as compared to the original linear system (1) above).

In this work, we represent the satellites formation flight topology by a connected directed graph, namely the *formation digraph*, in which each vertex represents a satellite and each edge connecting two vertices (satellites) represents a relative state measurement of the sink satellite with respect to the source satellite. We assume that the formation digraph is connected, which implies that one can determine all the $N(N-1)/2$ relative states (N is the number of satellites). Also, we assume that there exists the possibility of an all-to-all communication among the satellites, although our goal is to optimize and minimize the amount of information that is being exchanged among the satellites.

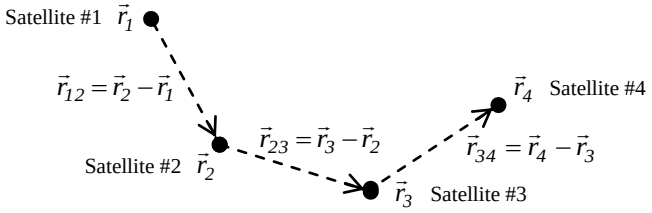

Figure 2. A formation of four satellites *#1*, *#2*, *#3*, and *#4* with relative output measurements (dashed edges).

For illustrative purposes only and without loss of generality, let us consider the fault estimation problem for the simple case of *4*-satellite formation with relative output measurements, which include the relative position vectors that are represented by the dashed edges in the formation digraph of Figure 2. In this *4*-satellite formation in deep space, we assume that the satellites *#1*, *#2*, and *#3* are subjected to actuator faults, and that satellite *#4* is healthy and whose dynamics *will be excluded* from the estimation procedure in the following derivations and analysis. We take the *x*-axis relative position $x_{ij} = x_j - x_i$ and the *x*-axis relative velocity $v_{x_{ij}} = v_{x_j} - v_{x_i}$ between the faulty satellites *#1* and *#2* (*i=1, j=2*) and the faulty satellites *#2* and *#3* (*i=2, j=3*) as the *relative-state vector* $(x_{12}, v_{x_{12}}, x_{23}, v_{x_{23}})^T$. Moreover, we define the permanent fault parameters f_{x_1}, f_{x_2}, and f_{x_3} as the three additional (fault) states having the dynamics $\dot{f}_{x_1} = 0$, $\dot{f}_{x_2} = 0$, and $\dot{f}_{x_3} = 0$, respectively. We augment these additional (fault) states with the relative-state vector to construct the *fault-augmented relative-state vector* as $\theta^a_{x_{123}} = (f_{x_1}, x_{12}, v_{x_{12}}, f_{x_2}, x_{23}, v_{x_{23}}, f_{x_3})^T$. By taking the time derivative of the fault-augmented relative-state vector $\theta^a_{x_{123}}$, the *fault-augmented relative-measurement relative-state model* is now governed by

$$\dot{\theta}^a_{x_{123}}(t)=\underbrace{\begin{bmatrix} 0 & 0 & 0 & 0 & 0 & 0 & 0 \\ 0 & 0 & 1 & 0 & 0 & 0 & 0 \\ -\frac{u_{x_1}}{m_1} & 0 & 0 & \frac{u_{x_2}}{m_2} & 0 & 0 & 0 \\ 0 & 0 & 0 & 0 & 0 & 0 & 0 \\ 0 & 0 & 0 & 0 & 0 & 1 & 0 \\ 0 & 0 & 0 & +\frac{u_{x_2}}{m_2} & 0 & 0 & \frac{u_{x_3}}{m_3} \\ 0 & 0 & 0 & 0 & 0 & 0 & 0 \end{bmatrix}}_{A_{x_{123}}(t)}\theta^a_{x_{123}}(t)+\underbrace{\begin{bmatrix} 0 & 0 & 0 \\ 0 & 0 & 0 \\ -\frac{\bar{b}_{x_1}}{m_1} & \frac{\bar{b}_{x_2}}{m_2} & 0 \\ 0 & 0 & 0 \\ 0 & \frac{0}{\bar{b}_{x_2}} & 0 \\ 0 & -\frac{\bar{b}_{x_2}}{m_2} & \frac{\bar{b}_{x_3}}{m_3} \\ 0 & 0 & 0 \end{bmatrix}}_{B_{x_{123}}}\underbrace{\begin{bmatrix} u_{x_1}(t) \\ u_{x_2}(t) \\ u_{x_3}(t) \end{bmatrix}}_{u_{x_{123}}}+W_{x_{123}} \tag{3}$$

$$z^a_{x_{123}}(t)=\underbrace{\begin{bmatrix} 0 & 1 & 0 & 0 & 0 & 0 & 0 \\ 0 & 0 & 0 & 0 & 1 & 0 & 0 \end{bmatrix}}_{C_{x_{123}}}\theta^a_{x_{123}}(t)+V_{x_{123}} \tag{4}$$

where the vectors $W_{x_{123}}$ and $V_{x_{123}}$ are the external disturbances and the sensor measurement noise, respectively, and the sub-matrices are clearly identified.

The objective is now to design estimation filters for the system that is governed by the equations (3)-(4). First, we need to verify the observability of the above system which is clearly in an equivalent form of a bilinear system as can be seen from the following representation

$$\dot{\theta}^a_{x_{123}}(t)=\underbrace{\begin{bmatrix} 0 & 0 & 0 & 0 & 0 & 0 & 0 \\ 0 & 0 & 1 & 0 & 0 & 0 & 0 \\ 0 & 0 & 0 & 0 & 0 & 0 & 0 \\ 0 & 0 & 0 & 0 & 0 & 0 & 0 \\ 0 & 0 & 0 & 0 & 0 & 1 & 0 \\ 0 & 0 & 0 & 0 & 0 & 0 & 0 \\ 0 & 0 & 0 & 0 & 0 & 0 & 0 \end{bmatrix}}_{A_0}\theta^a_{x_{123}}(t)+\underbrace{\begin{bmatrix} 0 & 0 & 0 \\ 0 & 0 & 0 \\ -\frac{\bar{b}_{x_1}}{m_1} & \frac{\bar{b}_{x_2}}{m_2} & 0 \\ 0 & 0 & 0 \\ 0 & 0 & 0 \\ 0 & -\frac{\bar{b}_{x_2}}{m_2} & \frac{\bar{b}_{x_3}}{m_3} \\ 0 & 0 & 0 \end{bmatrix}}_{B_{x_{123}}}\underbrace{\begin{bmatrix} u_{x_1}(t) \\ u_{x_2}(t) \\ u_{x_3}(t) \end{bmatrix}}_{u_x}+W_{x_{123}}$$

$$+u_{x_1}\underbrace{\begin{bmatrix} 0 & 0 & 0 & 0 & 0 & 0 & 0 \\ 0 & 0 & 0 & 0 & 0 & 0 & 0 \\ -\frac{1}{m_1} & 0 & 0 & 0 & 0 & 0 & 0 \\ 0 & 0 & 0 & 0 & 0 & 0 & 0 \\ 0 & 0 & 0 & 0 & 0 & 0 & 0 \\ 0 & 0 & 0 & 0 & 0 & 0 & 0 \\ 0 & 0 & 0 & 0 & 0 & 0 & 0 \end{bmatrix}}_{A_1}\theta^a_{x_{123}}(t)+u_{x_2}\underbrace{\begin{bmatrix} 0 & 0 & 0 & 0 & 0 & 0 & 0 \\ 0 & 0 & 0 & 0 & 0 & 0 & 0 \\ 0 & 0 & 0 & \frac{1}{m_2} & 0 & 0 & 0 \\ 0 & 0 & 0 & 0 & 0 & 0 & 0 \\ 0 & 0 & 0 & 0 & 0 & 0 & 0 \\ 0 & 0 & 0 & -\frac{1}{m_2} & 0 & 0 & 0 \\ 0 & 0 & 0 & 0 & 0 & 0 & 0 \end{bmatrix}}_{A_2}\theta^a_{x_{123}}(t)+u_{x_3}\underbrace{\begin{bmatrix} 0 & 0 & 0 & 0 & 0 & 0 & 0 \\ 0 & 0 & 0 & 0 & 0 & 0 & 0 \\ 0 & 0 & 0 & 0 & 0 & 0 & 0 \\ 0 & 0 & 0 & 0 & 0 & 0 & 0 \\ 0 & 0 & 0 & 0 & 0 & 0 & 0 \\ 0 & 0 & 0 & 0 & 0 & 0 & \frac{1}{m_3} \\ 0 & 0 & 0 & 0 & 0 & 0 & 0 \end{bmatrix}}_{A_3}\theta^a_{x_{123}}(t)$$

$$z^a_{x_{123}}(t)=\underbrace{\begin{bmatrix} 0 & 1 & 0 & 0 & 0 & 0 & 0 \\ 0 & 0 & 0 & 0 & 1 & 0 & 0 \end{bmatrix}}_{C_{x_{123}}}\theta^a_{x_{123}}(t)+V_{x_{123}}$$

In the bilinear system above, the state dynamic equation $\dot{\theta}^a_{x_{123}}(t)=A_0\theta^a_{x_{123}}(t)+B_{x_{123}}\,u_x+W_{x_{123}}+u_{x_1}A_1\theta^a_{x_{123}}(t)+u_{x_2}A_2\theta^a_{x_{123}}(t)$

$+u_{x_3} A_3 \theta^a_{x_{123}}(t)$ contains the multiplicative state-input (or bilinear) terms $u_{x_1} A_1 \theta^a_{x_{123}}(t)$, $u_{x_2} A_2 \theta^a_{x_{123}}(t)$, and $u_{x_3} A_3 \theta^a_{x_{123}}(t)$ (that is why the above system is classified as a bilinear system) as well as state and input (or linear) terms $A_0 \theta^a_{x_{123}}(t)$ and $B_{x_{123}} u_x$, respectively (that are common in linear systems).

By invoking results from the observability theorem of bilinear systems that is developed in [34] one can indeed show that the system given by equations (3)-(4) is observable since its observability matrix is full-rank, that is $rank(O(C_{x_{123}}, A_0, A_1, A_2, A_3)) = n = 7$, in which the observability matrix is defined according to

$$O(C_{x_{123}}, A_0, A_1, A_2, A_3) = col(C_{x_{123}}, C_{x_{123}}A_0, \ldots, C_{x_{123}}A_3, C_{x_{123}}A_0^2, C_{x_{123}}A_0A_1, \ldots, C_{x_{123}}A_0A_3, C_{x_{123}}A_1A_0, \ldots, C_{x_{123}}A_3^{n-1})$$

where the operator $col(.)$ implies that one stacks all the operand elements in one column with the same order. The above bilinear model is merely used to verify the observability of the system that is given by equations (3)-(4), which will be used in the following to design the estimation filters.

Since the fault-augmented model given by equations (3)-(4) is observable, it can be used to design a centralized Kalman filter (CKF) for estimating all the associated variables and states, namely f_{x_i}, x_{ij}, $v_{x_{ij}}$, and f_{x_j}. The matrix $A_{x_{123}}(t)$ in equation (3) is an overlapping-block-diagonal square matrix, which contains two blocks $A_{x_{12}}(t)$ and $A_{x_{23}}(t)$. A conventional CKF can be designed for the bilinear (or equivalently the linear time-varying (LTV)) model that is represented by the quadruple $(A_{x_{123}}(t), B_{x_{123}}, C_{x_{123}}, \mathbf{0}_{2\times 3})$ given by equations (3)-(4). The CKF estimator has two major drawbacks, namely

- Communication constraint: The CKF estimator requires full state communication exchanges among the satellites, albeit that the information availability will not remain robust to communication interruptions, dropouts and failures, and
- Error propagation: The CKF estimator requires an accurate centralized model of the entire satellite formation; whereas a local failure, uncertainty, or unmodeled dynamics can adversely affect the estimation performance of the entire formation.

In order to remedy the above major limitations and shortcomings, we are therefore motivated to propose and design reconfigurable distributed Kalman filters (RDKF) that can cooperate through a hybrid and switching framework. Our proposed RDKF approach is "distributed" in the sense that multiple local estimation filters (with information exchanges among them) will be utilized instead of a single centralized estimation filter. Moreover, our proposed RDKF approach is "reconfigurable" in the sense that a proper set of local estimation filters will be selected (by using a hybrid and switching framework) based on the information regarding the detected unmodeled dynamics, uncertainties, and disturbances. These issues are described formally next.

A. Reconfigurable Distributed Kalman Filters (RDKF)

In this part, we introduce our proposed *unconditional and conditional local estimation filters* as well as our proposed reconfigurable distributed Kalman filters (RDKF) that are developed and obtained through cooperation (information exchanges) among the local estimation filters.

Unconditional Local Estimation Filters:

Unconditional local estimation filters are introduced to tackle and resolve the communication constraint problem that is discussed above. An unconditional local estimation filter is a local Kalman filter that is to be implemented for each satellite #*i*, with the neighboring satellite #*j*, which is governed by the local linear time-varying (LTV) model as described below

$$\dot{\theta}^a_{x_{ij}}(t) = A_{x_{ij}}(t)\theta^a_{x_{ij}}(t) + B_{x_{ij}}u_{x_{ij}}(t) + W_{x_{ij}} + E^i_{x_{ij}}g_{x_i} + E^j_{x_{ij}}g_{x_j} \tag{5}$$

$$z^a_{x_{ij}}(t) = C_{x_{ij}}\theta^a_{x_{ij}}(t) + V_{x_{ij}} \tag{6}$$

where $\theta^a_{x_{ij}} = (f_{x_i}, x_{ij}, v_{x_{ij}}, f_{x_j})^T$ is the fault-augmented state with elements that are similarly defined in equations (3)-(4), except for the vectors $g_{x_i}(t)$ and $g_{x_j}(t)$ that represent the possible unmodeled dynamics and disturbances acting on satellites *#i* and *#j*, respectively, and $E^i_{x_{ij}}$ and $E^j_{x_{ij}}$ that denote the appropriate input vectors. The unmodeled dynamics and disturbances $g_{x_i}(t)$ can arise due to

- variations of the fault f_{x_i}, that is $g_{x_i}(t) = \dot{f}_{x_i} \neq 0$ as studied by the authors in [5], but that will not be considered in this paper by assuming that the fault signals are time-invariant or can be approximated as slowly time-varying signals (that is, $\dot{f}_{x_i} = 0$), or
- an unexpected communication delay τ that occurs while satellite *#i* is sending its control signal $u_{x_i}(t)$ to the other satellites, that is $g_{x_i}(t) = u_{x_i}(t-\tau) - u_{x_i}(t)$.

Our goal is to detect the presence of $g_{x_i}(t)$ and $g_{x_j}(t)$ in order to determine the reliability of the local model. If $g_{x_i}(t) = g_{x_j}(t) = 0$, then equation (5) is simply a subsystem of equation (3).

For illustrative purposes and without loss of generality let us consider the case $g_{x_1} = g_{x_2} = g_{x_3} = 0$, corresponding to the three faulty satellites *#1*, *#2*, and *#3* of the *4*-satellite formation that is shown in Figure 2. Figure 3a depicts the configuration of the two *unconditional* local estimation filters that represent reconfigurable distributed Kalman filters (RDKF) and are denoted by $EF_{x_{13}}(\hat{f}_{x_1}, \hat{f}_{x_3})$ and $EF_{x_{21}}(\hat{f}_{x_2}, \hat{f}_{x_1})$. These filters are basically conventional Kalman filters for the local model that is governed by equations (5)-(6) with the indices $(i=1, j=3)$ and $(i=2, j=1)$, respectively (Figure 3a). The bi-directional information exchange that is shown in Figure 3a is used for communicating the estimate of the common parameter $\hat{f}_{x_1}$ between the two local filters for subsequent date fusion [13]. This bidirectional information exchange is a source of error propagation when one is confronted with a local fault, uncertainty, or unmodeled dynamics, similar to the problems that one is confronted with in the CKF scheme in which the centralized overlapping-block-diagonal matrix structure of $A_{x_{123}}(t)$ (as characterized by equation (3)) propagates a local error to all the estimators of the system. For example, assume that in Figure 2 the satellites *#1* and *#3* are unmodeled dynamics and disturbance free (that is, $g_{x_1} = g_{x_3} = 0$), however satellite *#2* is subject to unmodeled dynamics and disturbances (that is, $g_{x_2} \neq 0$). In case of a bi-directional information exchange, as shown in Figure 3a, the unmodeled dynamics and disturbance $g_{x_2}(t)$ will affect the estimates of all the three fault signals f_{x_1}, f_{x_2} and f_{x_3}. In the following, the problem of error propagation will be tackled by using the *conditional* local estimation filters.

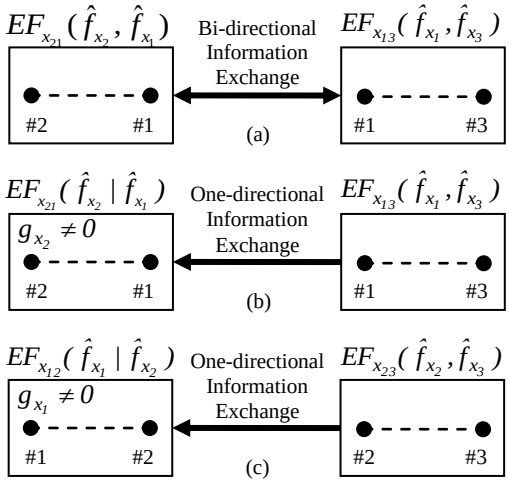

Figure 3. Reconfigurable distributed Kalman filter (RDKF) architectures in case of unmodeled dynamics and disturbances for the *3* faulty satellites of the *4*-satellite formation: (a) uncertainties are absent in all satellites, (b) uncertainties are present in satellite *#2*, and (c) uncertainties are present in satellite *#1*.

It should be noted that if an estimation filter is initialized with a positive definite covariance matrix for the estimation error, and if the covariance matrices of the system disturbance and measurement noise are positive semi-definite and bounded, then the covariance matrix of the estimation error remains positive definite and bounded for all time [40], [41].

Conditional Local Estimation Filters:

Conditional local estimation filters are introduced to remedy the error propagation problem that is discussed above. We need to control the direction of information exchange and data flow among the local filters. For example, the distributed structure that is shown in Figure 3b provides the necessary flexibility that one requires for restricting the effects of the unmodeled dynamics and disturbances $g_{x_2}(t)$ on the local fault estimate of satellite #*2*. This is achieved by implementing two local estimation filters, namely (a) the *unconditional* estimation filter $EF_{x_{13}}(\hat{f}_{x_1}, \hat{f}_{x_3})$, which is a conventional Kalman filter for the local model given by equations (5)-(6) with the indices $(i=1, j=3)$, and (b) the *conditional* estimation filter $EF_{x_{21}}(\hat{f}_{x_2} \mid \hat{f}_{x_1})$, which is a conventional Kalman filter with the indices $(i=2, j=1)$ for the local model that is governed by

$$\dot{\theta}^a_{x_{ij|j}}(t) = \overbrace{\begin{bmatrix} 0 & 0 & 0 \\ 0 & 0 & 1 \\ -\frac{u_{x_i}}{m_i} & 0 & 0 \end{bmatrix}}^{A_{x_{ij|j}}(t)} \theta^a_{x_{ij|j}}(t) + \overbrace{\begin{bmatrix} 0 & 0 \\ 0 & 0 \\ \frac{-\bar{b}_{x_i}}{m_i} & \frac{\bar{b}_{x_j} + f_{x_j}}{m_j} \end{bmatrix}}^{B_{x_{ij|j}}(t)} u_{x_{ij}}(t) + E^i_{x_{ij|j}} g_{x_i} + E^j_{x_{ij|j}} g_{x_j} \tag{7}$$

$$z^a_{x_{ij}}(t) = \underbrace{\begin{bmatrix} 1 & 0 & 0 \end{bmatrix}}_{C_{x_{ij|j}}(t)} \theta^a_{x_{ij|j}}(t) \tag{8}$$

where $\theta^a_{x_{ij|j}} = (f_{x_i}, x_{ij}, v_{x_{ij}})^T$ is the fault-augmented state and $E^i_{x_{ij|j}}$ and $E^j_{x_{ij|j}}$ denote the appropriate input vectors.

The unconditional estimation filter $EF_{x_{13}}(\hat{f}_{x_1}, \hat{f}_{x_3})$ estimates the fault signals f_{x_1} and f_{x_3} by using the relative measurement $z_{x_{13}} = z_{x_{12}} + z_{x_{23}}$, as shown in Figure 3b. The information on the estimate of f_{x_1} is then sent from $EF_{x_{13}}(\hat{f}_{x_1}, \hat{f}_{x_3})$ to

$EF_{x_{21}}(\hat{f}_{x_2} \mid \hat{f}_{x_1})$. This is shown by a solid arrow line in Figure 3b. The conditional estimation filter $EF_{x_{21}}(\hat{f}_{x_2} \mid \hat{f}_{x_1})$ estimates the fault signal f_{x_2} based on the information on f_{x_1} that it receives through an exchange with the unconditional estimation filter $EF_{x_{13}}(\hat{f}_{x_1}, \hat{f}_{x_3})$. This communication is the manifestation and representation of the *cooperative* nature of our proposed scheme for estimating the fault parameters. Through the above *cooperative scheme*, the unmodeled dynamics and disturbances $g_{x_2}(t)$ can only be guaranteed to affect the local estimate $\hat{f}_{x_2}$.

Remark 1. In the fault diagnosis literature, estimation methods belong to as one class of fault detection techniques [35]. In this paper, we use estimation filters to explicitly estimate the faults and implicitly detect them (in fact a fault is detected if it is estimated to be nonzero). The faults are augmented to the states of the system as governed by equations (5)-(6), where the faults are considered as part of the overall system states. In other words, they are considered as additional (fault) states that do not affect the dynamics of the system through an external input channel (as in the case of unmodeled dynamics and disturbances). Therefore, estimation filters are used to estimate the additional (fault) states, in contrast to standard approaches in the literature which are used to detect the faults (by using detection filters). On the other hand, the detection filters are only used for the purpose of detecting the uncertainties and disturbances, which affect the dynamics of the system through an external input channel. In order for the detection filters to distinguish between the unmodeled disturbances and modeled dynamics (and for improving the filters robustness), thresholds can be selected by using the Monte Carlo approach in which simulations are conducted for a number of scenarios that include random unmodeled dynamics and disturbances with specified ranges. In this manner, the thresholds are chosen so that the unmodeled disturbances can now be distinguished from the modeled dynamics, and hence can be used to improve the fault estimates as provided by the estimation filters.

The cooperative estimation strategy that is depicted in Figure 3 is mainly concerned with the following two tasks:

- detection of possible unmodeled dynamics and disturbances $g_{x_i}(t) \neq 0$, and
- estimation of the fault signals $f_{x_i}(t)$ based on the information on the unmodeled dynamics and disturbances $g_{x_i}(t)$.

For each of the above two problems, we offer a proposition below to address the issue.

Proposition 1. Consider an *N*-satellite formation flight that is represented by the set S. Using local detection filters it is possible to determine the set S_D, which is defined as the set of all satellites subjected to unmodeled dynamics and disturbances, if at least *2* satellites are unmodeled-disturbance free (that is, $n(S - S_D) \geq 2$ where $n(.)$ denotes the cardinality of the set).

Proof. In order to design the local detection filters, let us first consider the extended dynamical model that is given by equations (5)-(6). The structure of our proposed local Kalman detection filter $DF_{x_{ij}}$ is now specified according to

$$\dot{\hat{\theta}}^a_{x_{ij}}(t) = A_{x_{ij}}(t)\hat{\theta}^a_{x_{ij}} + B_{x_{ij}} u_{x_{ij}}(t) + K_{x_{ij}}(t)(z^a_{x_{ij}}(t) - \hat{z}^a_{x_{ij}}(t))$$

$$\hat{z}^a_{x_{ij}}(t) = C_{x_{ij}} \hat{\theta}^a_{x_{ij}}$$

where $K_{x_{ij}}(t)$ denotes the Kalman filter gain matrix. Let us select the residual error as $R_{x_{ij}}(t) = M(z^a_{x_{ij}}(t) - \hat{z}^a_{x_{ij}}(t))$, with an appropriate definition for the matrix M as conventionally determined in the fault diagnosis literature. When $g_{x_i} = g_{x_j} = 0$, the residual is in a neighborhood around zero (that is, $R_{x_{ij}}(t) = 0$). By proper selection of the threshold value, one can detect either a nonzero g_{x_i} or g_{x_j} by observing that the residual has exceeded the selected threshold bound for a sufficient duration of time.

Therefore, either g_{x_i} or g_{x_j} can force the residual error to exceed and cross over the threshold, and therefore it is not possible to isolate these signals based on the detection filters alone. Consequently, one needs to monitor all the residual errors within the formation in order to isolate the satellites that have unmodeled dynamics and disturbances.

Consider now the following logical definitions

$$G_{x_i} = 0 \quad \equiv \quad g_{x_i} = 0$$

$$G_{x_i} = 1 \quad \equiv \quad g_{x_i} \neq 0$$

$$R_{x_{ij}} = 0 \quad \equiv \quad residual\ of\ the\ DF_{x_{ij}}\ does\ not\ exceed\ the\ threshold$$

$$R_{x_{ij}} = 1 \quad \equiv \quad residual\ of\ the\ DF_{x_{ij}}\ exceeds\ the\ threshold\ permanently$$

The logical functional relation $R_{x_{ij}} \equiv G_{x_i} \vee G_{x_j}$ holds according to the definitions above. In other words, we have

$$(a)\ \ IF\ \ n(S_D) = N \quad \Rightarrow \quad \forall i,\ G_{x_i} = 1 \quad \Rightarrow \quad \forall i, j,\ R_{x_{ij}} = 1$$

$$(b)\ \ IF\ \ n(S_D) = N-1 \quad \Rightarrow \quad \exists! i,\ G_{x_i} = 0,\ \forall k \neq i,\ G_{x_k} = 1 \quad \Rightarrow \quad \forall i, j,\ R_{x_{ij}} = 1$$

$$(c)\ \ IF\ \ n(S_D) \leq N-2 \quad \Rightarrow \quad \exists i, j,\ G_{x_i} = G_{x_j} = 0 \quad \Rightarrow \quad R_{x_{ij}} = 0 \quad \Rightarrow \quad \forall k \notin \{i, j\} \begin{cases} k \notin S_D & R_{x_{ik}} = 0\ (R_{x_{jk}} = 0) \\ k \in S_D & R_{x_{ik}} \neq 0\ (R_{x_{jk}} \neq 0) \end{cases}$$

The above can clearly demonstrate that one needs at least two unmodeled-disturbance free satellites to identify the set S_D and this completes the proof of the proposition. ■

Following the above result on the set S_D, next we introduce our proposed estimation *reconfiguration* scheme in which a proper set of distributed conditional and unconditional estimation filters are selected to constrain the adverse effects of the unmodeled dynamics and disturbances on the local state estimates and prevent them from propagating to the neighboring satellite states.

Proposition 2. Given an *N*-satellite formation flight system, assume that at least *2* satellites (*#i* and *#j*) are unmodeled-disturbance free so that faults can be isolated by invoking the detection filters according to the Proposition 1. The Algorithm 1 presented below provides a procedure for reconfiguring the state estimation scheme by using distributed conditional and unconditional estimation filters. Using this algorithm the adverse effects of a given nonzero unmodeled dynamics and disturbances $g_{x_k} \neq 0$ are guaranteed to be constrained to only the corresponding satellite *#k* and will not propagate to the entire formation.

Table 1. Algorithm 1 for reconfiguration of the state estimation scheme.

Algorithm 1. Consider a set of *N* satellites that are denoted by $S = \{s_1, \ldots s_N\}$. Assume that the associated formation flight digraph is connected.

(i) START: Specify the set S_D ($S_D \subset S$), which is defined as the set of all satellites with unmodeled dynamics and disturbances, by using the distributed local detection filters as given in Proposition 1. It should be noted that at least two satellites are unmodeled-disturbance free (that is $n(S_D) \leq N-2$ where $n(.)$ denotes the *cardinality* of the set).

(ii) For each satellite $s_i \in S - S_D$, choose a satellite $s_j \in S - S_D$ ($j \neq i$) to be used in the corresponding unconditional filter $EF_{x_{ij}}(\hat{f}_{x_i}, \hat{f}_{x_j})$.

(iii) For each satellite $s_k \in S_D$, choose a satellite $s_j \in S - S_D$ to be used in the corresponding conditional filter $EF_{x_{kj}}(\hat{f}_{x_k} \mid \hat{f}_{x_j})$; END.

Proof. Assume that the two satellites *#i* and *#j* are identified according to the Proposition 1 to be unmodeled-disturbance free ($i, j \in S - S_D$). The unconditional local estimation filter $EF_{x_{ij}}(\hat{f}_{x_i}, \hat{f}_{x_j})$ can be employed to estimate the fault signals f_{x_i} and f_{x_j} without being exposed to the effects of the unmodeled-disturbances $g_{x_k} \neq 0$. The fault f_{x_k} that is injected in the satellite *k* with an unmodeled disturbance can be estimated by either the conditional estimation filter $EF_{x_{ki}}(\hat{f}_{x_k} \mid \hat{f}_{x_i})$ or $EF_{x_{kj}}(\hat{f}_{x_k} \mid \hat{f}_{x_j})$. The conditional estimation filter $EF_{x_{ki}}(\hat{f}_{x_k} \mid \hat{f}_{x_i})$ (or $EF_{x_{kj}}(\hat{f}_{x_k} \mid \hat{f}_{x_j})$) estimates the severity of f_{x_k} by taking information on the estimate $\hat{f}_{x_i}$ (or $\hat{f}_{x_j}$) of the unmodeled-disturbances free satellite *#i* (or *#j*) through a communication with the unconditional estimation filter $EF_{x_{ij}}(\hat{f}_{x_i}, \hat{f}_{x_j})$. In other words, the conditional estimation filter $EF_{x_{ki}}(\hat{f}_{x_k} \mid \hat{f}_{x_i})$ (or $EF_{x_{kj}}(\hat{f}_{x_k} \mid \hat{f}_{x_j})$) merely estimates the local fault signal f_{x_k} and not f_{x_i} (or f_{x_j}). Therefore, the effects of the unmodeled-disturbances g_{x_k} will not propagate to the entire formation state estimators through the fault estimates $\hat{f}_{x_i}$ and $\hat{f}_{x_j}$. This completes the proof of the proposition.

■

In order to generalize our reconfigurable distributed estimation approach, in the next section we propose a hybrid and switching framework. In this framework, each mode represents a certain estimation scheme as well as a specific communication topology among the local estimation filters (as per Proposition 2). The transitions among the modes are conditioned on the residuals that are generated by the local detection filters (as per Proposition 1).

B. Cooperation of Estimators in a Hybrid and Switching Framework

In general, a linear approximation of a nonlinear system can be better represented by a hybrid structure, which is constructed by using discrete modes corresponding to various operating conditions and linear continuous-time models. In the literature a number of estimation methods based on the interactive multiple model (IMM) or the probabilistic hybrid automata (PHA) have been proposed to address the state estimation problem in hybrid systems [36]. In our work, we consider the formation system as being represented by a non-hybrid continuous-time model. The system is to be estimated by using distributed and local estimation filters. Cooperation among these estimation filters will require different communication topologies, which are individually considered as particular modes that are integrated into a hybrid model framework. In other words, we represent our proposed cooperative fault estimation framework through a hybrid and switching model in which each mode represents a certain cooperative scheme that is achieved among the local filters (as per Proposition 2).

In order to set up our hybrid and switching framework for cooperative fault estimation, we first start by allocating the states of the formation flight system to the local estimation and detection filters based on topological considerations. For sake of illustrative purposes we describe this concept with an example of *3* faulty satellites *#1*, *#2*, and *#3* (from the *4*-satellite formation as shown in Figure 2). Figure 4 shows the configuration of the *3* faulty satellites (having only relative measurements) among the 3 distributed local detection filters, 3 unconditional and 6 conditional local estimation filters, where the superscript ij in $\hat{f}_{x_i}^{ij}$ indicates that the fault estimate $\hat{f}_{x_i}^{ij}$ is accomplished by the conditional estimation filter $EF_{x_{ij}}(\hat{f}_{x_i}^{ij} \mid \hat{f}_{x_j}^{ij})$ or the unconditional estimation filter $EF_{x_{ij}}(\hat{f}_{x_i}^{ij}, \hat{f}_{x_j}^{ij})$. It should be noted that the healthy satellite *#4* is omitted from Figure 4 as well as the subsequent discussions since this satellite is healthy, and hence it does not require an actuator fault estimator.

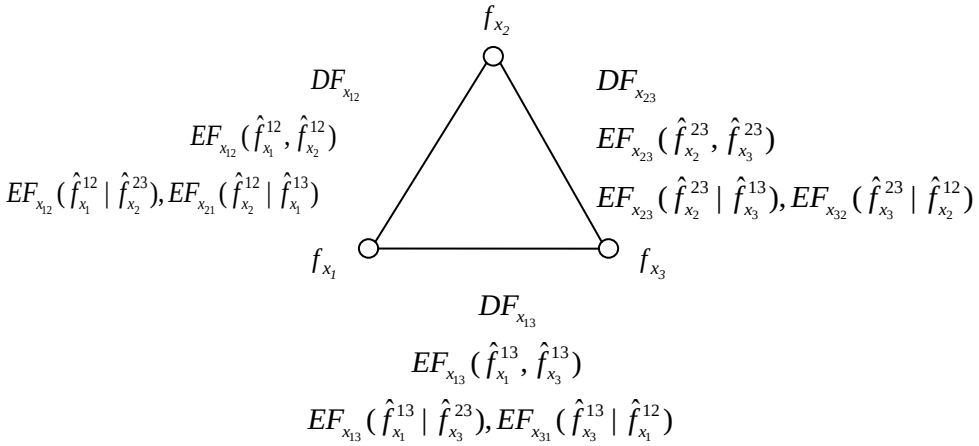

Figure 4. The allocation of the local detection filters (DFs) and the local estimation filters (EFs) among the *3* faulty satellites #*1*, #*2*, and #*3* (from the *4*-satellite formation shown in Figure 2).

Let us now introduce the following notations and definitions to characterize the cooperation among the reconfigurable distributed estimation filters that are suggested by the Propositions 1 and 2. The residual error signal $R_{x_{ij}}$ is generated by the three detection filters $DF_{x_{ij}}$ (as indicated in Figure 4) according to Proposition 1. Through construction of these three residuals additional conditions that are denoted by $\varsigma(m_i)$ are obtained below that determine the transition (switching) to a mode #*i*, in which the distributed (3 unconditional and 6 conditional) local estimation filters (as indicated in Figure 4) are reconfigured according to Proposition 2. In Proposition 2, it was assumed that at least *2* satellites are unmodeled-disturbance free, that is $n(S_D) \le N-2$ as explained in the Algorithm 1. Therefore, for the case of *3* faulty satellites #*1*, #*2*, and #*3* in Figure 4 one can distinguish four modes, namely mode #*0* with $S_D = \{\}$, mode #*1* with $S_D = \{s_1\}$, mode #*2* with $S_D = \{s_2\}$, and mode #*3* with $S_D = \{s_3\}$, where the condition $n(S_D) \le N-2 = 3-2 = 1$ is satisfied in all modes. These four modes are formally defined next.

Mode #0. Transition to this mode is conditioned on $\varsigma(m_0) = \{R_{x_{12}} = R_{x_{13}} = R_{x_{23}} = 0\}$, which implies that no unmodeled-disturbances is present in the formation satellites. Therefore, the two distributed unconditional filters $EF_{x_{12}}(\hat{f}_{x_1}^{12}, \hat{f}_{x_2}^{12})$ and $EF_{x_{13}}(\hat{f}_{x_1}^{13}, \hat{f}_{x_3}^{13})$ are employed to estimate all the system states and parameters. The two estimates of the common parameter $\hat{f}_{x_1}$ are then fused [13] according to $\hat{f}_{x_1} = \rho_{x_1}^{12}\hat{f}_{x_1}^{12} + \rho_{x_1}^{13}\hat{f}_{x_1}^{13}$, where $0 < \rho_{x_1}^{12}, \rho_{x_1}^{13} < 1$ and $\rho_{x_1}^{12} + \rho_{x_1}^{13} = 0$. This mode is depicted in Figure 3a.

Mode #1. Transition to this mode is conditioned on $\varsigma(m_1) = \{R_{x_{12}} \neq 0, R_{x_{13}} \neq 0, R_{x_{23}} = 0\}$, which implies that the unmodeled-disturbances g_{x_1} is present ($g_{x_1} \neq 0$) in satellite #*1*. Therefore, the unconditional filter $EF_{x_{23}}(\hat{f}_{x_2}^{23}, \hat{f}_{x_3}^{23})$ and either the conditional filter $EF_{x_{12}}(\hat{f}_{x_1}^{12} \mid \hat{f}_{x_2}^{23})$ or $EF_{x_{13}}(\hat{f}_{x_1}^{13} \mid \hat{f}_{x_3}^{23})$ can be employed to cooperatively estimate all the system states and parameters. This mode is depicted in Figure 3c.

Mode #2. Transition to this mode is conditioned on $\varsigma(m_2) = \{R_{x_{12}} \neq 0, R_{x_{23}} \neq 0, R_{x_{13}} = 0\}$, which implies that the unmodeled-

disturbances g_{x_2} is present ($g_{x_2} \neq 0$) in satellite *#2*. Therefore, the unconditional filter $EF_{x_{13}}(\hat{f}_{x_1}^{13}, \hat{f}_{x_3}^{13})$ and either the conditional filter $EF_{x_{21}}(\hat{f}_{x_2}^{12} \mid \hat{f}_{x_1}^{13})$ or $EF_{x_{23}}(\hat{f}_{x_2}^{23} \mid \hat{f}_{x_3}^{13})$ can be employed to cooperatively estimate all the system states and parameters. This mode is depicted in Figure 3b.

Mode #3. Transition to this mode is conditioned on $\varsigma(m_3) = \{R_{x_{13}} \neq 0, R_{x_{23}} \neq 0, R_{x_{12}} = 0\}$, which implies that the unmodeled-disturbances g_{x_3} is present ($g_{x_3} \neq 0$) in satellite *#3*. Therefore, the unconditional filter $EF_{x_{12}}(\hat{f}_{x_1}^{12}, \hat{f}_{x_2}^{12})$ and either the conditional filter $EF_{x_{31}}(\hat{f}_{x_3}^{13} \mid \hat{f}_{x_1}^{12})$ or $EF_{x_{32}}(\hat{f}_{x_3}^{23} \mid \hat{f}_{x_2}^{12})$ can be employed to cooperatively estimate all the system states and parameters.

We are now in a position to integrate the above four modes for the *3* faulty satellites to construct a hybrid and switching representation of our proposed reconfigurable distributed estimation filters as shown in Figure 5. In this figure, certain condition $\varsigma(m_i)$, $i = 1,2,3,4$ should be satisfied in order to switch to the mode *#i*, in which combinations of 6 conditional and 3 unconditional local estimation filters are employed. As explained in the four modes above, the condition $\varsigma(m_i)$ is constructed by using the residuals of the 3 local detection filters. Formally analyzing and designing a HL supervisor for our hybrid and switching estimation framework is beyond the scope of this work, although it has been studied by the authors in [6] by using a discrete-event system (DES) [27] approach for the general case of linear time-invariant (LTI) systems. Finally, the sensitivity of our proposed fault estimation scheme with respect to the probabilities of "mis-detect" and "false-alarm" is also beyond the scope of this work and is left as a topic of future research.

Once the low-level fault recovery (LLFR) module completes the cooperative fault estimation task, the fault estimates are then utilized by the controllers in the LLFR. As the number of satellites in the fleet increases and the communication resources become constrained, the motivation for implementing a semi-decentralized FLFR strategy becomes more justifiable and crucial. Our proposed decentralized control recovery methodology is now discussed and developed in the next section.

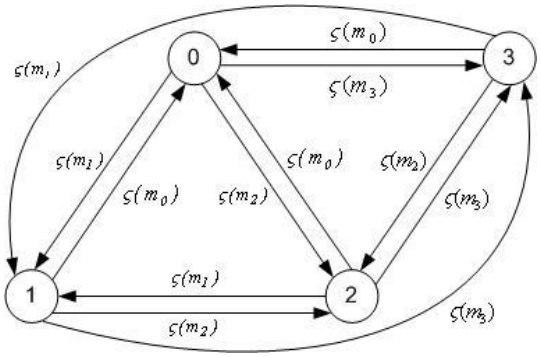

Figure 5. The hybrid and switching estimation model that is employed for the *3* faulty satellites.

IV. SEMI-DECENTRALIZED RECOVERY CONTROLLERS BY THE LLFR MODULE

Consider now a four-satellite formation flight system, whose formation digraph is shown in Figure 6. In practice, it is not always possible to ensure and provide a one-to-all inter satellite relative measurements. Therefore, one needs to avoid and handle the so-called cascade of accumulating measurement error effects. The measurement topology adopted highly depends on (a) the formation geometry, and (b) the resource availability (measurement sensors). As an illustration of (a) formation geometry, when all the satellites are lined up in a straight line, it is not possible to achieve a one-to-all measurement topology due to lack of visibility and field of view obstacles from the outer satellite to all the others. As an example of (b) resource availability, a one-to-

all measurement scheme requires the availability of a large number of sensors that are not cost-wise practical. In this paper, the one-to-all relative measurements are not required to be available among the satellites, and therefore the sensors are assumed to be sufficiently accurate to avoid the cascade accumulating measurement error effects.

Based on our previous discussions in Sections II and III, the model of the satellite *#i* shown in Figure 6 is approximated by a double integrator [1], [2] for each of the three axes as follows

$$\begin{aligned} m_i \ddot{x}_i &= b_{x_i} u_{x_i} + d_x \\ m_i \ddot{y}_i &= b_{y_i} u_{y_i} + d_y \\ m_i \ddot{z}_i &= b_{z_i} u_{z_i} + d_z \end{aligned} \tag{9}$$

where the environmental disturbances are represented by $(d_x, d_y, d_z)^T$ (the above representation is similar to the model given by equation (1)), and the other parameters and variables are defined in Section II.

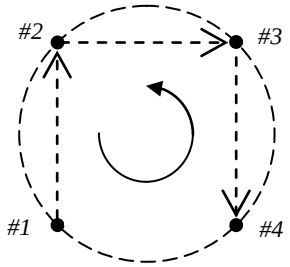

Figure 6. A four-satellite formation flight system.

For sake of simplicity in the derivations, the following analysis ignores the effects of disturbances for now. However, these effects are subsequently analyzed and taken into account in the next section. Moreover, as in the previous discussions, given that the three axes dynamics are decoupled, we only consider the dynamics of the *x*-axis although the results can trivially be extended to the *y*- and *z*-axes dynamics. The dashed line edges shown in Figure 6 represent the system output measurements. In order to avoid output redundancy, three outputs (corresponding to the three dashed lines) are chosen. For each dashed line, the corresponding output tracking error and its first two time derivatives are formally defined

$$\begin{aligned} e_{ij} &= x_{ij} - x_{ij}^d \\ \dot{e}_{ij} &= \dot{x}_{ij} - \dot{x}_{ij}^d \\ \ddot{e}_{ij} &= \frac{b_{x_j}}{m_j} u_{x_j} - \frac{b_{x_i}}{m_i} u_{x_i} - \ddot{x}_{ij}^d \end{aligned} \tag{10}$$

where $x_{ij} = x_j - x_i$ is the relative position between the satellites *#i* and *#j*, and x_{ij}^d is their desired relative reference trajectory. In the compact matrix form the second derivatives of the output errors for the four-satellite formation system can be expressed as follows

$$\begin{bmatrix}\ddot{e}_{12}\\ \ddot{e}_{23}\\ \ddot{e}_{34}\end{bmatrix}=\underbrace{\begin{bmatrix}\frac{-b_{x_1}}{m_1} & \frac{b_{x_2}}{m_2} & 0 & 0\\ 0 & \frac{-b_{x_2}}{m_2} & \frac{b_{x_3}}{m_3} & 0\\ 0 & 0 & \frac{-b_{x_3}}{m_3} & \frac{b_{x_4}}{m_4}\end{bmatrix}}_{J}\begin{bmatrix}u_{x_1}\\ u_{x_2}\\ u_{x_3}\\ u_{x_4}\end{bmatrix}-\begin{bmatrix}\ddot{x}_{12}^{d}\\ \ddot{x}_{23}^{d}\\ \ddot{x}_{34}^{d}\end{bmatrix} \tag{11}$$

In order to investigate the controllability of the system given by equation (11) under the loss of effectiveness actuator faults, let us express the above system in the standard state space form as follows

$$\frac{d}{dt}\begin{bmatrix}e_{12}\\ \dot{e}_{12}\\ e_{23}\\ \dot{e}_{23}\\ e_{34}\\ \dot{e}_{34}\end{bmatrix}=\underbrace{\begin{bmatrix}0&1&0&0&0&0\\ 0&0&0&0&0&0\\ 0&0&0&1&0&0\\ 0&0&0&0&0&0\\ 0&0&0&0&0&1\\ 0&0&0&0&0&0\end{bmatrix}}_{A_{tot}}\begin{bmatrix}e_{12}\\ \dot{e}_{12}\\ e_{23}\\ \dot{e}_{23}\\ e_{34}\\ \dot{e}_{34}\end{bmatrix}+\underbrace{\begin{bmatrix}0 & 0 & 0 & 0\\ \frac{-b_{x_1}}{m_1} & \frac{b_{x_2}}{m_2} & 0 & 0\\ 0 & 0 & 0 & 0\\ 0 & \frac{-b_{x_2}}{m_2} & \frac{b_{x_3}}{m_3} & 0\\ 0 & 0 & 0 & 0\\ 0 & 0 & \frac{-b_{x_3}}{m_3} & \frac{b_{x_4}}{m_4}\end{bmatrix}}_{B_{tot}}\begin{bmatrix}u_{x_1}\\ u_{x_2}\\ u_{x_3}\\ u_{x_4}\end{bmatrix}-\begin{bmatrix}0\\ \ddot{x}_{12}^{d}\\ 0\\ \ddot{x}_{23}^{d}\\ 0\\ \ddot{x}_{34}^{d}\end{bmatrix}$$

The standard controllability matrix of the above system is defined as

$$C(A_{tot},B_{tot})=\begin{bmatrix}B_{tot} & A_{tot}B_{tot} & A_{tot}^{2}B_{tot} & \cdots & A_{tot}^{n}B_{tot}\end{bmatrix} \qquad (n=6)$$

For all values of the loss-of-effectiveness fault parameters f_{x_i} $(i=1,2,3,4)$ in $b_{x_i}=\bar{b}_{x_i}+f_{x_i}$ (as in equation (2)), the controllability matrix remains full rank if we have $0<b_{x_i}\le\bar{b}_{x_i}$ or equivalently $-\bar{b}_{x_i}<f_{x_i}\le 0$. Therefore, the overall formation system that is subjected to the loss-of-effectiveness fault parameters satisfying $-\bar{b}_{x_i}<f_{x_i}\le 0$ $(i=1,2,3,4)$ will always remain controllable.

Remark 2. As evident from equation (11), the dynamical equation of the formation flight system is in the linear time-invariant form from the control point of view. It should also be noted that the fault-augmented relative-measurement relative-state model that is given by equations (3)-(4) was earlier shown to be in the form of linear time-varying model and bilinear model from the estimation and the observability perspectives, respectively.

In deep space, instead of using imprecise measurements of absolute states x_i and $\dot{x}_i$, due to the availability of high precision autonomous formation flying (AFF) sensors [37] one can alternatively consider measuring the relative states x_{ij} and $\dot{x}_{ij}$ and then use them in the formation feedback loop. In order to avoid redundant measurements, we assume that the formation digraph is connected. To each edge $x_{ij}=x_j-x_i$ representing the relative state measurement of the satellite #*j* with respect to the satellite #*i*, we assign two parameters $\alpha_{ij}\in R$ and $\beta_{ij}\in R$ in order to design our semi-decentralized controllers [42].

Let us now define the following general vectors for the case of N satellites with a connected digraph

$$\ddot{x}^{d}\overset{\Delta}{=}\begin{bmatrix}\vdots\\ \ddot{x}_{ij}^{d}\\ \vdots\end{bmatrix}_{(N-1)\times 1},\quad e\overset{\Delta}{=}\begin{bmatrix}\vdots\\ e_{ij}\\ \vdots\end{bmatrix}_{(N-1)\times 1},\quad X\overset{\Delta}{=}\begin{bmatrix}\vdots\\ \begin{bmatrix}e_{ij}\\ \dot{e}_{ij}\end{bmatrix}\\ \vdots\end{bmatrix}_{2(N-1)\times 1},\quad \alpha\overset{\Delta}{=}\begin{bmatrix}\vdots\\ \alpha_{ij}\\ \vdots\end{bmatrix}_{(N-1)\times 1},\quad \beta\overset{\Delta}{=}\begin{bmatrix}\vdots\\ \beta_{ij}\\ \vdots\end{bmatrix}_{(N-1)\times 1} \tag{12}$$

where the elements $\ddot{x}_{ij}^{d}$, e_{ij}, α_{ij}, β_{ij}, and $\begin{bmatrix} e_{ij} & \dot{e}_{ij} \end{bmatrix}^T$ are on the same corresponding rows of the vectors $\ddot{x}^d$, e, α, β, and X, respectively. The states $\ddot{x}_{ij}^{d}$ and e_{ij} were introduced earlier in equation (10). In the compact matrix form, the tracking error dynamics can be expressed according to

$$\ddot{e} = Ju - \ddot{x}^d \tag{13}$$

where the input vector u and the matrix J are given by

$$u = \begin{bmatrix} u_{x_1} \\ \vdots \\ u_{x_N} \end{bmatrix} \quad , \quad J(i,j) = \begin{cases} \dfrac{b_{x_j}}{m_j} & if\ \exists k \in \{1,\ldots,N\};\ e_{[i]} = e_{kj} \\ \dfrac{-b_{x_j}}{m_j} & if\ \exists k \in \{1,\ldots,N\};\ e_{[i]} = e_{jk} \\ 0 & otherwise \end{cases}$$

with the notation that $e_{[i]}$ denotes the *i*-th element of the vector e in equation (12). For example, in the special case of Figure 6, the error dynamics is given by equation (11). The dynamics of individual satellites are coupled through their relative state measurements. In the following, a semi-decentralized control strategy is proposed and implemented in order to meet the restrictive communication constraints that are imposed on the formation system due to the availability of only local relative state measurements. Motivated by conventional linear control design techniques, a semi-decentralized controller is designed in which the control signal u_{x_i} of satellite #*i* is specified in terms of the local relative state measurements and the desired trajectories of its neighboring satellites.

To design the semi-decentralized controllers, we first start by incorporating the actuator faults estimates that are obtained from the previous section into the control channels as follows

$$u = diag(m_1, m_2, \ldots, m_N)\, diag\left(\hat{b}_{x_1}^{-1}, \hat{b}_{x_2}^{-1}, \ldots, \hat{b}_{x_N}^{-1}\right)(u_d + u_s) \tag{14}$$

where the actuator gain b_{x_i} is now replaced by its estimate $\hat{b}_{x_i}$ (that is, $\hat{b}_{x_i} = \bar{b}_{x_i} + \hat{f}_{x_i}$), where the estimate $\hat{f}_{x_i}$ of the fault f_{x_i} is given by equation (2). Moreover, it easily follows that $\hat{b}_{x_i} = b_{x_i}$ when the system is fault free or when one has an accurate estimate of f_{x_i}. The control terms u_d and u_s are the *desired acceleration tracking* control and the *stabilizing* control signals, respectively, that are specified as follows

$$u_d = A(\alpha)\ddot{x}^d \quad , \quad u_s = B(\beta)\Lambda X$$

where the tracking error state X and the desired acceleration state $\ddot{x}^d$ are defined in equation (12), and

$$\Lambda = diag\left(\begin{bmatrix} -\lambda_0 & -\lambda_1 \end{bmatrix}, \ldots, \begin{bmatrix} -\lambda_0 & -\lambda_1 \end{bmatrix}\right)_{(N-1)\times 2(N-1)} \quad , \quad A(\alpha) = \begin{bmatrix} A_1^T(\alpha) \\ \vdots \\ A_N^T(\alpha) \end{bmatrix}_{N\times(N-1)} \quad , \quad B(\beta) = \begin{bmatrix} B_1^T(\beta) \\ \vdots \\ B_N^T(\beta) \end{bmatrix}_{N\times(N-1)} \tag{15}$$

with $A(\alpha)$ and $B(\beta)$ denoting the design matrices that depend on the parameters α and β.

In order to finally construct our proposed semi-decentralized controllers one needs to appropriately select the above matrices such that their structure is sufficiently sparse. In other words, one needs to generate the control signal u_{x_i} of satellite #*i* merely in terms of the information that is available from the local relative state measurements and the desired trajectories of its neighboring satellites. Towards this end, the matrices $A(\alpha)$ and $B(\beta)$ are selected and specified next.

For obtaining the vectors $A_i(\alpha)$, $i=1,\ldots,N$ in equation (15), an arbitrary satellite, let's say s_r is chosen as the reference and is assigned with $A_r(\alpha)=\alpha$. For each α_{ij}, an associated vector T_{ij}^{α} is defined according to $\alpha^T T_{ij}^{\alpha}=\alpha_{ij}$. Let us define the set $N(r)$ as the index set of all the satellites s_j that are neighbors to the satellite s_r, that is

$$N(r)=\{\, j \mid \exists k \in \{1,\ldots,N-1\}; e_{[k]}=e_{rj} \ \text{or} \ e_{[k]}=e_{jr} \,\} \tag{16}$$

where as before $e_{[k]}$ denotes the *k*-th element of the vector e in equation (12).

For any given neighbor satellite s_j ($j \in N(r)$), we evaluate

$$A_j(\alpha)=A_r(\alpha)+T_{rj}^{\alpha}$$

with the consideration that $T_{rj}^{\alpha}=-T_{jr}^{\alpha}$. This neighboring derivation can be accomplished by induction through the relative-measurement digraph of the entire formation so that all the vectors $A_i(\alpha)$, $i=1,\ldots,N$ are specified to form the matrix $A(\alpha)$ in equation (15).

For deriving $B_i^T(\beta)=\begin{bmatrix} B(i,1) & \cdots & B(i,N-1) \end{bmatrix}$ in equation (15), we take

$$B(i,k)=\begin{cases} \beta_{ij}-1 & \text{if } \exists\, j \in N(i); e_{[k]}=e_{ij} \\ \beta_{ji} & \text{if } \exists\, j \in N(i); e_{[k]}=e_{ji} \\ 0 & \text{otherwise} \end{cases}$$

As an illustration, in the special case of the formation flight that is shown in Figure 6, the matrices $A(\alpha)$ and $B(\beta)$ have the following structures

$$A(\alpha)=\begin{bmatrix} \alpha_{12}-1 & \alpha_{23}-1 & \alpha_{34}-1 \\ \alpha_{12} & \alpha_{23}-1 & \alpha_{34}-1 \\ \alpha_{12} & \alpha_{23} & \alpha_{34}-1 \\ \alpha_{12} & \alpha_{23} & \alpha_{34} \end{bmatrix}, \quad B(\beta)=\begin{bmatrix} \beta_{12}-1 & 0 & 0 \\ \beta_{12} & \beta_{23}-1 & 0 \\ 0 & \beta_{23} & \beta_{34}-1 \\ 0 & 0 & \beta_{34} \end{bmatrix} \tag{17}$$

In the following, the stability of the overall formation flight system is shown formally by using the semi-decentralized controller that is given by equation (14).

Theorem 1. Consider either a fault free satellite formation flight system (13) (that is, $b_{x_i}=\bar{b}_{x_i}$ or $f_{x_i}\equiv 0$) or the formation flight system that is equipped with an accurate fault estimation scheme (that is, $\hat{b}_{x_i}=b_{x_i}$), then by proper choice of the design parameters (λ_0,λ_1) there exists a nonempty set for the vector $\beta \in R^{N-1}$ such that the closed-loop system given by equations (13)-(14) is input-output stable for all the values of $\alpha \in R^{N-1}$.

Proof. First, it should be pointed out that by substituting the control law u from equation (14) into equation (13), the control signal u_d cancels out the terms $\ddot{x}^d$ and $A(\alpha)$, which results in the closed-loop system. The control u_s forms the nominal (disturbance free) closed-loop dynamical system that is given by $\dot{X}=(I+\Delta_d(\beta))\Phi X$. This closed-loop dynamical system can equivalently be represented by an alternative system S and the controller CON, that are characterized as follows

$$S:\begin{cases} \dot{X}=\Phi X+U \\ Y=\Phi X \end{cases}, \quad CON: U=\Delta_d(\beta)Y$$

where

$$\Phi = diag\left\{ \begin{bmatrix} 0 & 1 \\ -\lambda_0 & -\lambda_1 \end{bmatrix}_i \right\}_{i=1}^{N-1}$$

and $\Delta_d(\beta)$ is a square matrix whose elements are either zero or function of β.

The system S is controllable and observable, and the matrix Φ is stable (that is all its poles are in the left-half of the s-plane) for all $\lambda_0 > 0$ and $\lambda_1 > 0$. Using the results from the small-gain theorem [38], and by taking

$$\gamma_1 = \sup_{\omega \in R} \sigma_{max}[\Phi(sI - \Phi)^{-1}]$$

a sufficient condition for stability of the closed-loop system is given by $\beta \in D_\beta = \left\{ \beta \in R^{N-1} \mid ||\Delta_d(\beta)||_\infty < 1/\gamma_1 \right\}$. The set D_β is nonempty if the pair (λ_0, λ_1) is chosen properly, that is

$$(\lambda_0, \lambda_1) \in D_{(\lambda_0,\lambda_1)} = \left\{ (\lambda_0, \lambda_1) \in R^2 \mid \gamma_1(\lambda_0, \lambda_1) < 1/\min_\beta ||\Delta_d(\beta)||_\infty \right\}$$

This completes the proof of the theorem. ■

For the special case of the formation flight system that is shown in Figure 6, the matrix $\Delta_d(\beta)$ has the following structure

$$\Delta_d(\beta) = \begin{bmatrix} 0 & 0 & 0 & 0 & 0 & 0 \\ 0 & 0 & 0 & \beta_{23} - 1 & 0 & 0 \\ 0 & 0 & 0 & 0 & 0 & 0 \\ 0 & -\beta_{12} & 0 & 0 & 0 & \beta_{34} - 1 \\ 0 & 0 & 0 & 0 & 0 & 0 \\ 0 & 0 & 0 & -\beta_{23} & 0 & 0 \end{bmatrix} \tag{18}$$

and the stability condition becomes

$$\beta \in D_\beta = \left\{ \beta \in R^3 \middle| max(|\beta_{23} - 1|, |\beta_{12}| + |\beta_{34} - 1|, |\beta_{23}|) < \frac{1}{\gamma_1} \right\}$$

Since $0.5 < min(|\beta_{23} - 1|, |\beta_{12}| + |\beta_{34} - 1|, |\beta_{23}|)$ holds always, the set D_β is nonempty by the proper choice of (λ_0, λ_1) as follows

$$(\lambda_0, \lambda_1) \in D_{(\lambda_0,\lambda_1)} = \left\{ (\lambda_0, \lambda_1) \in R^2 \middle| \gamma_1(\lambda_0, \lambda_1) = \sup_{\omega \in R} \sigma_{max}[\Phi(sI - \Phi)^{-1}] < 2 \right\}$$

In the next section, it is shown that an imprecise estimate of an actuator fault signal can significantly impact the performance of the overall formation flying system. This performance degradation will be detected by the HL supervisor and, subsequently, the FLFR module is activated. We will then propose a semi-decentralized cooperative fault accommodation scheme in the FLFR module by designing a controller that is similar to equation (14) and which guarantees that the desired mission error specifications in presence of possible estimation inaccuracies and biases are nevertheless maintained and satisfied.

V. Cooperative Fault Accommodation by the FLFR Module

Consider the four-satellite formation flight system that is depicted in Figure 6. Assume that the satellite *#2* is faulty and is partially recovered by the low-level fault recovery (LLFR) system due to the presence of a biased and inaccurate fault estimate. In other words, satellite *#2* tracks the desired trajectory with an error bound of r, which is greater than the mission error specification given by e_s (that is $r > e_s$).

The purpose of the formation-level fault recovery (FLFR) module is to ensure that by restraining the control efforts of satellite

#2, at the expense of higher control efforts from other satellites *#1*, *#3* and *#4*, the mission tracking error bound r is reduced to satisfy the design specifications of the formation flight (that is $r < e_s$). Our main objective here is to propose a framework and suggest guidelines for optimally accomplishing the FLFR module performance requirements.

Let us now consider a loss-of-effectiveness fault in satellite *#i* actuator and assume that the LLFR module has estimated the severity of this fault, which is biased and imprecise, that is $\hat{f}_{x_i} = f_{x_i} + \varepsilon$, or equivalently $\hat{b}_{x_i} = b_{x_i} + \varepsilon$, where ε is unknown but bounded (that is $|\varepsilon| < B_\varepsilon$) with B_ε a known bound. This biased estimate will result in overall formation performance degradations that are subsequently detected by the HL supervisor. The supervisor then activates the FLFR module in order to satisfy the desired mission error specifications.

In the following, we investigate the stability and convergence of an *N*-satellite formation flying system by using the semi-decentralized controller that is given by equation (14) and is subject to the fact that the fault estimate in satellite *#i* actuator is biased. Our main result of this section is stated by the following theorem.

Theorem 2. Let the actuator of the satellite *#i* be subject to a loss effectiveness fault, and let the corresponding fault parameter estimate be biased such that $\hat{b}_{x_i} = b_{x_i} + \varepsilon$, where ε is unknown but bounded ($|\varepsilon| < B_\varepsilon$) and B_ε is a known bound. Using the semi-decentralized control scheme that is given by equation (14) it can be shown that:

(a) for proper choices of the design parameters $(\lambda_0, \lambda_1) \in D_{(\lambda_0,\lambda_1)}$ given by equation (21) (shown below), there exists nonzero values for $\beta \in R^{N-1}$ given by equation (20) for the control law u_s that is defined in equation (14) such that the nominal (disturbance free) closed-loop system given by equations (13)- (14) is stable, and

(b) for the stabilized closed-loop system in (a) there exists nonzero values for $\alpha \in R^{N-1}$ given by equation (24) for the control signal u_d that is defined in equation (14) such that the norm of the tracking error X remains smaller than the predefined specification given by e_s.

Proof. By substituting the control law u from equation (14) into equation (11) the resulting closed-loop system is obtained as

$$\dot{X} = (I + \Delta_{d\varepsilon,i})\Phi X + \overline{D}_{d,i}(t) \tag{19}$$

where $\Delta_{d\varepsilon,i}(\beta,\varepsilon)$ is a square matrix that depends on β and ε, and

$$\overline{D}_{d,i}(t) = \frac{\varepsilon}{\hat{b}_i} T_i A_i^T(\alpha)\ddot{x}^d(t)$$

in which the vector $T_i \in R^{2(N-1)}$ is defined as follows

$$T_i(k) = \begin{cases} 1 & if \ \exists j \in N(i); X_{[k]} = \dot{e}_{ij} \\ -1 & if \ \exists j \in N(i); X_{[k]} = \dot{e}_{ji} \\ 0 & otherwise \end{cases}$$

Similar to the proof of Theorem 1, by using the results from the small-gain theorem and by taking

$$\gamma_1 = \sup_{\omega \in R} \sigma_{max}[\Phi(sI - \Phi)^{-1}]$$

a sufficient condition for stability of the closed-loop system is governed by

$$\beta \in D'_\beta = \left\{ \beta \in R^{N-1} \,\middle|\, \forall \varepsilon \in [-B_\varepsilon, B_\varepsilon], \| \Delta_{d\varepsilon,i}(\beta,\varepsilon) \|_\infty < 1/\gamma_1 \right\} \tag{20}$$

The set D'_β is nonempty if the design parameters (λ_0, λ_1) are chosen properly, that is

$$(\lambda_0,\lambda_1)\in D'_{(\lambda_0,\lambda_1)}=\left\{(\lambda_0,\lambda_1)\in R^2\,\middle|\,\gamma_1(\lambda_0,\lambda_1)<1/\min_{\beta\in R^3,\varepsilon<B_\varepsilon}\|\Delta_{d\varepsilon,i}(\beta,\varepsilon)\|_\infty\right\} \tag{21}$$

This completes the proof of part (a).

For part (b), we start from the fact that the closed-loop system is already shown to be stable according to the results from part (a). Denoting $\Phi_{dclp,i}=(I+\Delta_{d\varepsilon,i})\Phi$ in equation (19), the tracking error X is now governed by the dynamical system $\dot{X}(t)=\Phi_{dclp,i}X(t)+\overline{D}_{d,i}(t)$, whose Laplace transform is given by

$$X(s)=(sI-\Phi_{dclp,i})^{-1}\overline{D}_{d,i}(s)=G_{d,i}(s)\overline{D}_{d,i}(s)$$

(assuming that the initial conditions are neglected) where $G_{d,i}(s)$ is the transfer function matrix. By using the definition of $\overline{D}_{d,i}(t)$ from equation (19), we get

$$X(s)=\frac{\varepsilon}{\hat{b}_i}G_{d,i}(s)T_iA_i^T(\alpha)\mathcal{L}\{\ddot{x}^d(t)\}$$

where $\mathcal{L}\{.\}$ denotes the Laplace transform of a given signal. Let us denote $A_i(\alpha)=\|A_i(\alpha)\|\hat{A}_i(\alpha)$, where $\hat{A}_i(\alpha)$ is the normalized $A_i(\alpha)$. We now obtain

$$X(s)=\frac{\varepsilon}{\hat{b}_i}G_{d,i}(s)T_i\|A_i(\alpha)\|\hat{A}_i^T(\alpha)\mathcal{L}\{\ddot{x}^d\}$$

Taking

$$H_{d,i}(\hat{A}_i(\alpha))\overset{\Delta}{=}\frac{1}{\hat{b}_i}\sup_{t\in R^+,|\varepsilon|<B_\varepsilon,\beta\in D'_\beta}\left|G_{d,i}(t)T_i*\left(\hat{A}_i^T(\alpha)\ddot{x}^d(t)\right)\right| \tag{22}$$

where "$*$" denotes the convolution operator, we get

$$|X(t)|\le|\varepsilon|H_{d,i}(\hat{A}_i(\alpha))\|A_i(\alpha)\|\overset{\Delta}{=}B_{X,i} \tag{23}$$

In order for the norm of the tracking error X be smaller than the specification e_s, a conservative solution based on equation (23) can be obtained as follows

$$\max|\varepsilon|H_{d,i}(\hat{A}_i(\alpha))\|A_i(\alpha)\|\le e_s\quad\Rightarrow\quad\|A_i(\alpha)\|\le\frac{e_s}{B_\varepsilon H_{d,i}(\hat{A}_i(\alpha))}$$

The desired domain for the parameter α can therefore be specified which is given by

$$D'_\alpha=\left\{\alpha\in R^{N-1}\,\middle|\,\|A_i(\alpha)\|\le\frac{e_s}{B_\varepsilon H_{d,i}(\hat{A}_i(\alpha))}\right\} \tag{24}$$

This completes the proof of part (b) and of the theorem. ■

For the special case of the formation flight system that is depicted in Figure 6, the matrix $\Delta_{d\varepsilon,2}(\beta,\varepsilon)$ and the vector T_2 (satellite #*2* is assumed faulty) have the following structures

$$\Delta_{d\varepsilon,2} = \begin{bmatrix} 0 & 0 & 0 & 0 & 0 & 0 \\ 0 & -\frac{\varepsilon}{\hat{b}_2}\beta_{12} & 0 & \left(1-\frac{\varepsilon}{\hat{b}_2}\right)(\beta_{23}-1) & 0 & 0 \\ 0 & 0 & 0 & 0 & 0 & 0 \\ 0 & \left(\frac{\varepsilon}{\hat{b}_2}-1\right)\beta_{12} & 0 & \frac{\varepsilon}{\hat{b}_2}(\beta_{23}-1) & 0 & \beta_{34}-1 \\ 0 & 0 & 0 & 0 & 0 & 0 \\ 0 & 0 & 0 & -\beta_2 & 0 & 0 \end{bmatrix} \quad , \quad T_2 = \begin{bmatrix} 0 & -1 & 0 & 1 & 0 & 0 \end{bmatrix}^T$$

Consequently, the stability condition in Theorem 2 becomes

$$\beta \in D'_\beta = \left\{ \beta \in R^3 \,\middle|\, \forall \varepsilon \in [-B_\varepsilon, B_\varepsilon] \ , \ max\left[\left|\frac{\varepsilon}{\hat{b}_2}\beta_{12}\right| + \left|\left(1-\frac{\varepsilon}{\hat{b}_2}\right)(\beta_{23}-1)\right| , \left|\left(\frac{\varepsilon}{\hat{b}_2}-1\right)\beta_{12}\right| + \left|\frac{\varepsilon}{\hat{b}_2}(\beta_{23}-1)\right| + |\beta_{34}-1| \ , \ |\beta_{23}| \right] < \frac{1}{\gamma_1} \right\}$$

Let us now assume that an external (environmental) disturbance D_{ext} that is bounded by B_{ext} (that is $||D_{ext}|| < B_{ext}$) is applied to the system that is given by equation (19) as $\dot{X} = (I + \Delta_{d\varepsilon,i})\Phi X + \overline{D}_{d,i}(t) + D_{ext}$. Following along similar steps as those used in the proof of Theorem 2, equation (23) can be re-written as follows

$$|X(t)| \leq B_{X,i} + B_{ext,i} = B_{tot} \tag{25}$$

where

$$B_{ext,i} \stackrel{\Delta}{=} \sup_{t \in R^+, |\varepsilon| < B_\varepsilon, \beta \in D'_\beta} \int_{t'=-\infty}^{+\infty} \left| G_{d,i}(t-t')T_i \right| B_{ext} dt' > 0$$

One immediate conclusion from the above is that one cannot certainly get a better (smaller) error bound than $B_{ext,i}$.

The domain D'_α that is given by equation (24) yields a conservative estimate. Therefore, it may be preferable to deal with this problem from a probabilistic perspective. We assume that the probability distribution function of the estimation error ε is known and is given by $f_\varepsilon(m)$ where $m \in [-\infty \ \infty]$. Our objective is to specify and determine the parameter vector α such that the probability of violating the error specification e_s is less than a predefined value π ($0 \leq \pi << 1$), namely $P(|X(t)| < e_s) > 1 - \pi$.

By taking into account the definition of B_{tot} from equation (25), we have

$$P(|X(t)| < e_s) = P(|X(t)| < e_s \mid B_{tot} < e_s) P(B_{tot} < e_s) + P(|X(t)| < e_s \mid B_{tot} > e_s) P(B_{tot} > e_s)$$

Since $|X(t)| < B_{tot}$, we have $P(|X_i(t)| < e_s \mid B_{tot} < e_s) = 1$. Therefore, the above equation is equivalent to

$$P(|X(t)| < e_s) = P(B_{tot} < e_s) \quad + P(|X(t)| < e_s \mid B_{tot} > e_s) P(B_{tot} > e_s)$$

Since the second right-hand term in the above expression is positive, we conclude that

$$P(|X(t)| < e_s) \quad > \quad P(B_{tot} < e_s)$$

or equivalently, replacing for $B_{X,i}$ and B_{tot} from equations (23) and (25), respectively, we get

$$P(|X(t)| < e_s) > P\left(|\varepsilon| H_{d,i}(\hat{A}_i(\alpha)) ||A_i^T(\alpha)|| + B_{ext,i} < e_s \right) = P(\varepsilon^- < \varepsilon < \varepsilon^+)$$

where

$$\varepsilon^+ = -\varepsilon^- = \frac{e_s - B_{ext,i}}{H_{d,i}(\hat{A}_i(\alpha)) ||A_i^T(\alpha)||}.$$

Therefore, the problem reduces to that of finding the vector α which satisfies the equality

$$\int_{m=\varepsilon^-}^{\varepsilon^+} f_\varepsilon(m)dm \quad = \quad 1-\pi$$

If the information about the probability distribution function of the estimation error ε is not available, one conventional and practical solution would be to assume that it is uniformly distributed over the interval $[-B_\varepsilon \; B_\varepsilon]$ and is given by

$$f_\varepsilon(m) = \begin{cases} \dfrac{1}{2B_\varepsilon} & -B_\varepsilon < m < B_\varepsilon \\ 0 & otherwise \end{cases} \tag{26}$$

Consequently, the following equation needs to be solved for α, that is $\int_{m=\varepsilon^-}^{\varepsilon^+} \frac{1}{2B_\varepsilon} dm \quad = \quad 1-\pi \quad \Rightarrow \quad \frac{\varepsilon^+ - \varepsilon^-}{2B_\varepsilon} = 1-\pi$.

The above expression yields the desired set of feasible solutions for α as follows

$$D'_\alpha = \left\{ \alpha \in R^{N-1} \middle| \; ||A_i^T(\alpha)|| \leq \frac{e_s}{B_\varepsilon(1-\pi)H_{d,i}(\hat{A}_i(\alpha))} \right\} \tag{27}$$

The solution in equation (24) is a special case (the most conservative result corresponding to $\pi = 0$) of the solution in equation (27). It should be pointed out that one can improve the performance of the FLFR module by utilizing a more accurate probability distribution function instead of the uniform distribution function that is given in equation (26).

The limitation of our proposed FLFR scheme is that it can only accommodate at most one partially LL-recovered satellite in each of the *x*-, *y*-, and *z*-axes (that is at most 3 satellites simultaneously). If more than one satellite in each axis is partially LL-recovered, then the proposed solution would be to reduce $H_{d,i}(.)$ (as given by equation (22)) by decreasing the desired trajectory $\ddot{x}^d(t)$, which implies that one requires a new path planning procedure for the entire satellite formation. These scenarios are beyond the scope of the present work and will be investigated in future. In the next section, the effectiveness of our proposed strategy will be demonstrated in a number of simulation studies.

VI. Simulation Results

Consider the four-satellite deep space formation in the *xy*-plane as shown in Figure 6. The objective is a counter-clockwise rotation maneuver in the *xy*-plane with the frequency of $\omega = 0.1 \; (rad/s)$, such that the satellites always maintain a square shape with the side lengths of $200 \; (m)$ and with an error specification of $e_s = 0.025 (m)$. The desired formation outputs are the relative distances among the neighboring satellites. The major environmental disturbance in deep space is solar pressure [39]. It is calculated according to the formula $F = C_R IS / C$, where $C_R = 1.0$ is the solar radiation coefficient, I is the solar radiation intensity, S is the area upon which solar radiation is forced, and $C = 3 \times 10^8 \; (m/s)$ is the speed of light. By taking $I = 3000 (Watt/m^2)$ and $S = 1 (m^2)$ the solar pressure is computed to be in the order of $10^{-5} (N)$. This is represented as an additive zero-mean white Gaussian process with the variance of $10^{-5} (N)$. For simulations, the sensor noise is also considered to be an additive zero-mean white Gaussian process with the variance of $10^{-4} \; (m^2)$.

A *20%* loss-of-effectiveness fault is applied to the *x*-axis actuator of satellites *#1*, *#2*, and *#3*. The corresponding fault parameter in satellite *#2* is estimated by the LLFR module within a *22%* relative error, that is $|\varepsilon_{x_2}| / b_{x_2} = |\hat{b}_{x_2} - b_{x_2}| / b_{x_2} = 0.22$, whereas the fault parameter in satellites *#1* and *#3* are estimated accurately. Using the low-

level (LL) recovery controller and the design parameters that are selected as $\lambda_0 = 2$ and $\lambda_1 = 3$ to satisfy $(\lambda_0, \lambda_1) \in D'_{(\lambda_0,\lambda_1)}$, we consider the following three simulation scenarios, namely (A), (B), and (C).

In scenario (A), all the satellites are fault free and the error specification $e_s = 0.025(m)$ is satisfied with a properly designed controller. In scenario (B), satellites *#1*, *#2*, and *#3* are faulty and the HL supervisor activates the LLFR module. This module estimates the actuator faults by using the cooperative estimators according to our proposed hybrid and switching framework and incorporates the estimates in the LLFR module controllers to fully recover all the satellites. However, satellite *#2* is assumed to be only partially recovered by the LLFR module due to a biased estimate of its fault, and consequently the overall mission error specification $e_s = 0.025(m)$ is violated. In scenario (C), the HL supervisor first detects this violation and consequently activates the FLFR module to cooperatively accommodate the partially LL-recovered satellite *#2* so that the overall mission error specifications can now be guaranteed. In the following, the above three scenarios are described and analyzed in more detail.

Scenario A. All the satellites are fault free

In this case, the semi-decentralized controller given by equation (14) is specified with the parameter $\alpha = (0.25, 0.50, 0.75)^T$. This selection is made by minimizing the energy of the input signal u_d according to the cost function

$$f_{cost}(.) = \int_{t=0}^{\infty} \left(u_d^T(t) u_d(t) \right) dt$$

The concluding result obtained yields $||A_2^T(\alpha)|| = 0.6124$. The vector $\beta = (0.3835, 0.5000, 0.6165)^T$ is chosen according to the condition given by Theorem 1. It can be shown that the maximum tracking error corresponding to the closed-loop system is indeed quite acceptable (namely, $error = 0.015\ m << 0.025m = e_s$). Figure 7a shows the *x*-axis cumulative control effort expensed which is defined according to

$$E_{xi}(t) = \int_{\tau=0}^{t} u_{xi}^2(\tau)\, d\tau \qquad (i = 1,2,3,4)$$

Scenario B. Satellites #1, #2, and #3 are faulty and the fault in satellite #2 is only partially recovered by the LLFR module

In this case, the HL supervisor activates the LLFR module which performs cooperative fault estimation according to our proposed hybrid and switching framework for the three faulty satellites *#1*, *#2*, and *#3* (from the *4*-satellite formation shown in Figure 2) based on the reconfiguration strategy that is introduced in Propositions 1 and 2 and illustrated in Figure 3. For each local Kalman filter estimator, we assume that the model disturbance ($W_{x_{ij}}$) and the sensor noise ($V_{x_{ij}}$) are zero-mean white Gaussian random processes with covariance matrices $Q = 10^{-5} I_{n \times n}$ and $R = 10^{-4} I_{m \times m}$, respectively, where I denotes an identity matrix and m and n are the dimensions of the system state and the output vectors, respectively.

In the time interval $T_{12} = [0\ \ 100]\ (sec)$, the LLFR module successfully performs the estimation task in mode *#0* of the hybrid and switching framework. Note that the notion of modes *#0, #1, #2*, and *#3* are defined for the three faulty satellites *#1*, *#2*, and *#3* (from the *4*-satellite formation shown in Figure 2) in Section III, and they are applicable to our case study in this section. Subsequently, at time $t \geq T_2 = 100\ (sec)$, satellite *#2* is exposed to additional permanent unknown disturbances and unmodeled dynamics $g_{x_2}(t)$ that affect the estimation performance. This uncertainty has arisen due to an unexpected communication delay that has occurred while satellite *#2* is sending its control signal $u_{x_2}(t)$ to the other satellites. In the simulations conducted this

uncertainty is represented by $g_{x_2}(t) = u_{x_2}(t-\tau) - u_{x_2}(t)$, where $\tau = 0.1\ (sec)$. In order to constrain the adverse effects of $g_{x_2}(t)$ on the local estimators and to prevent its effects on the estimates of all the states and parameters throughout the formation, at time T_2 the HL module (through a hybrid and switching framework) makes a decision to switch from mode *#0* to *#1* as described in more detail next.

We consider the following sequential simulation steps:

1. At time $T_1 = 0\ (sec)$ the estimation process is initiated in mode *#0* (as per the configuration that is shown in Figure 3a), and the estimate for the fault signal in satellite *#2* is shown in Figure 8. Similar results for the estimate of the fault signals in satellites #1 and #3 are obtained (not shown). The estimation performance corresponding to this mode is similar to that of a CKF but due to space limitations the simulation results are omitted.
2. In the time interval $T_{12} = [0\ \ 100]\ (sec)$, no uncertainties are present in the formation ($g_{x_i}(t) = 0$, $i = 1,\ldots,3$). This situation can be detected by monitoring the residual signals as shown in Figure 9. It can be concluded that the condition $\varsigma(m_0) = \{ R_{x_{12}} = R_{x_{13}} = R_{x_{23}} = 0 \}$ corresponding to mode *#0* is satisfied.
3. At time $T_2 = 100\ (sec)$, the uncertainty $g_{x_2}(t) = u_{x_2}(t-\tau) - u_{x_2}(t)$, as described earlier, is injected to the formation system. This event is detected by monitoring the residual signals that are shown in Figure 9 during the time interval $T_{23} = [100\ \ 200]\ (sec)$. It can be concluded that the condition $\varsigma(m_1) = \{ R_{x_{12}} \neq 0,\ R_{x_{23}} \neq 0,\ R_{x_{13}} = 0 \}$ to switch to mode *#2* is satisfied.
4. At time $T_2 = 100\ (sec)$ the estimation process switches to the mode *#2* (as per configuration shown in Figure 3b), and the estimates for the fault signals are now obtained as shown in Figures 10 and 11. The results for the satellite *#3* are very similar to those of satellite *#1* and are therefore not shown.

In order to demonstrate the significance and effectiveness of our proposed switching framework from mode *#0* to mode *#2* at time T_2, both the time intervals T_{12} and T_{23} are depicted in Figures 7-11. One can compare the T_{23}-interval estimation performance of mode *#0* in Figure 8 with that of mode *#2* in Figure 11. The results of this comparison are summarized in Table 2. In this table the means and variances of the fault signal estimation errors are indicated for the modes *#0* and *#1*. It can be clearly observed that by using our proposed reconfigurable distributed estimation scheme, the LLFR module has successfully made the right decision to switch from mode *#0* to mode *#2*.

The fault estimates are ultimately used in the semi-decentralized LLFR module controllers as given by equation (14), where the parameter vectors α and β are taken to be the same as those obtained in part (A). Figure 7b shows the *x*-axis cumulative control efforts of the LLFR module controllers. Since the fault estimate in satellite *#2* is biased, the maximum tracking error that is obtained in satellite *#2* is unacceptable (in other words, $error = 0.034\ \ m > 0.025m = e_s$), and hence the faulty satellite *#2* is partially recovered by the LLFR module, although the satellites *#1* and *#3* are fully recovered by this module. Therefore, in the next part (C) the HL supervisor is invoked to activate the FLFR module for performing cooperative fault accommodation among the four satellites in support of the partially LL-recovered satellite *#2*.

Scenario C. The partially LL-recovered satellite #2 is cooperatively accommodated by the FLFR module

When the semi-decentralized controller that is given by equation (14) is selected, the FLFR module modifies the parameter vector α by using the results of Theorem 2 such that $||A_2^T(\alpha)||$ is reduced from its initial value of 0.6124, as selected in parts

(A) and (B). The analytical (as per equation (27)) and the simulation (experimental) values for $||A_2^T(\alpha)||$ versus the maximum allowable tracking error e_s are sketched in Figure 12. This figure shows that the tracking error is reduced by decreasing $||A_2^T(\alpha)||$ in the FLFR module. To achieve the mission tracking error specification of $e_s = 0.025(m)$, the experimental curve in Figure 12 shows that the maximum required value of $||A_2^T(\alpha)||$ is $||A_2^T(\alpha)|| \models 0.4593$. On the other hand, based on analytical curves the maximum value of $||A_2^T(\alpha)||$ is estimated to be $||A_2^T(\alpha)|| \models 0.4712$ and $||A_2^T(\alpha)|| \models 0.3603$ corresponding to the violation probabilities of $\pi = 0.25$ and $\pi = 0.00$ (most conservative case), respectively. This result justifies the validity and effectiveness of our analytically estimated $||A_2^T(\alpha)||$ when compared with the experimental result of the desired $||A_2^T(\alpha)||$.

Figure 7c and Figure 7d depict the *x*-axis cumulative control efforts for the values of $||A_2^T(\alpha)|| \models 0.4712$ (for $\pi = 0.25$) and $||A_2^T(\alpha)|| \models 0.3603$ (for $\pi = 0.00$), respectively. Comparing the Figures 7c and 7d with the Figure 7b, one can conclude that the more $||A_2^T(\alpha)||$ is decreased by the FLFR module, the less satellite *#2* will use its control effort, and the more other satellites will allocate their control efforts to compensate for the deficiency of the satellite *#2*. This is an interesting interpretation of the FLFR module acting in support of the partially LL-recovered satellite *#2*.

Table 2. Comparison between the estimation performance of the reconfigurable distributed Kalman filter (RDKF) in mode *#0* with mode *#2* in the time interval $T_{23} = [100\ \ 200]\,(sec)$.

	Mean Estimation Error			Estimation Error Variance		
	f_{x_1}	f_{x_2}	f_{x_3}	f_{x_1}	f_{x_2}	f_{x_3}
Mode *#0*	*0.0363*	*0.0297*	*0.0311*	1.9×10^{-4}	1.1×10^{-4}	1.2×10^{-4}
Mode *#2*	*0.0004*	*0.0160*	*0.0003*	1.3×10^{-7}	2.5×10^{-4}	1.7×10^{-7}

VII. Conclusion

In this paper, a solution to the cooperative actuator fault estimation and accommodation in satellite formation flying was proposed and developed by introducing and considering a new hierarchical multi-level architecture. Two fault-recovery modules are designed, namely a low-level fault recovery (LLFR) and a formation-level fault recovery (FLFR). The LLFR module utilizes a hybrid and switching framework to cooperatively estimate the fault severities, and subsequently, utilizes these estimates in a conventional recovery controller. However, due to the inexact and biased estimate of the fault, the high level (HL) supervisor then detects the violations of the overall mission specifications, so that the FLFR module is activated. At the formation level, the partially LL-recovered faulty satellite is further accommodated by the entire formation, at the expense of the other healthy satellites allocating more control efforts to compensate for the deficiencies in the faulty satellite. The simulation results presented demonstrate that our proposed reconfigurable distributed Kalman filters (RDKF) for the hybrid and switching estimation framework could successfully limit and constrain the effects of unmodeled dynamics and uncertainties that are imposed on the local parameter estimators. This enables us to prevent the propagation of undesirable effects to the state estimators throughout the formation flight system. Moreover, as shown by simulations the FLFR module accommodates the faulty and partially LL-recovered satellites and ensures further improvements to the overall mission performance.

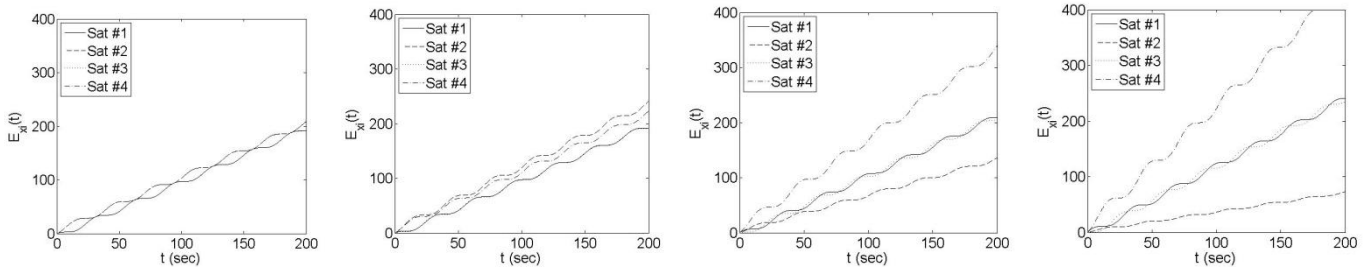

(a) (b) (c) (d)

Figure 7. The *x*-axis cumulative control effort for the scenarios where (a) all the satellites are fault free, (b) the faulty satellite #2 is partially LL-recovered with $|| A_2^T ||= 0.6124$, (c) the faulty satellite #2 invokes the HLFR module with $|| A_2^T ||= 0.4712$, and (d) the faulty satellite #2 invokes the HLFR module with $|| A_2^T ||= 0.3603$.

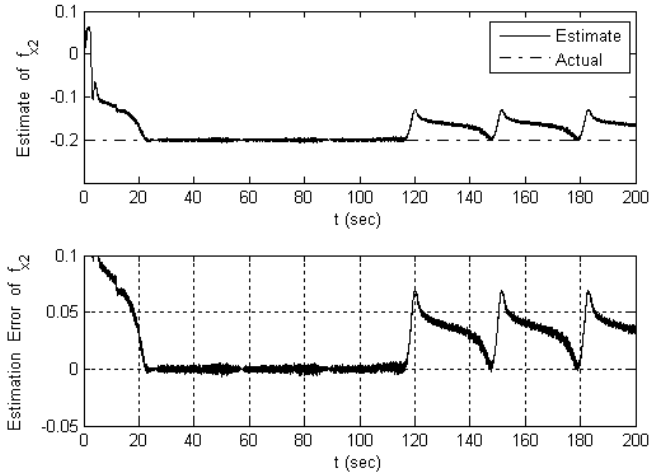

Figure 8. The actual, the estimated, and the estimation error of the fault in satellite #2 by using the reconfigurable distributed Kalman filter (RDKF) in mode *#0* (unconditional filters during the entire time interval).

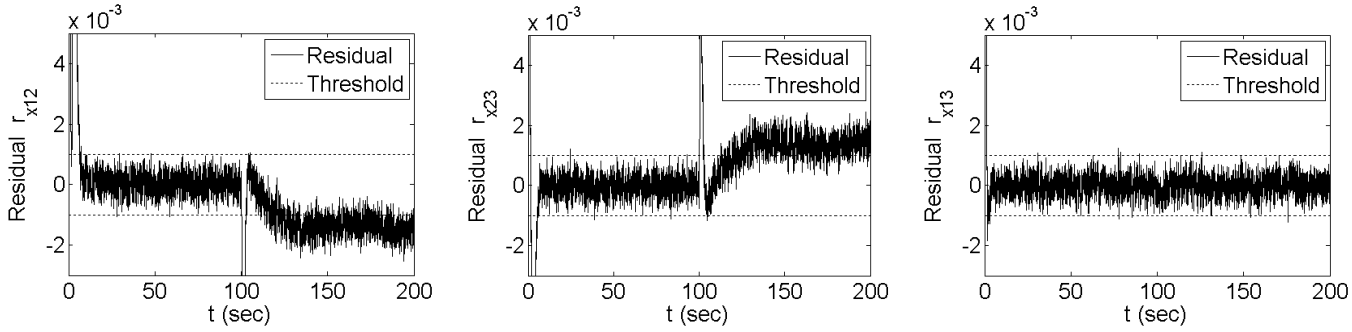

Figure 9. The residual signals corresponding to the three detection filters that are used by the LLFR module to determine the switching form mode *#0* to mode *#2* at time $T_2 = 100\,(sec)$, which are used to detect the unmodeled dynamics and disturbances of *3* faulty satellites *#1*, *#2*, and *#3* (of the *4*-satellite formation in Figure 2).

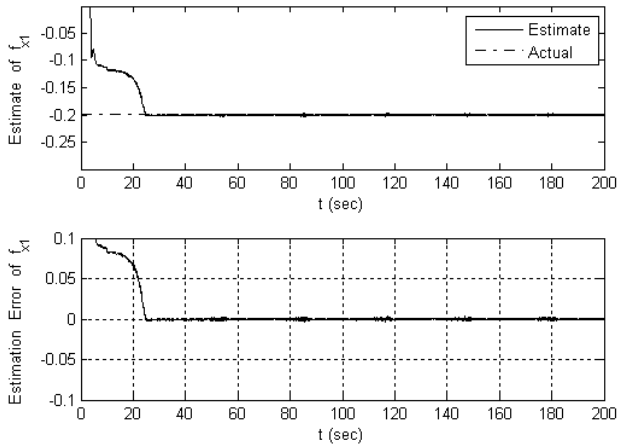

Figure 10. The actual, the estimated, and the estimation error of the fault in satellite #1 by using the reconfigurable distributed Kalman filter (RDKF) in mode *#2*.

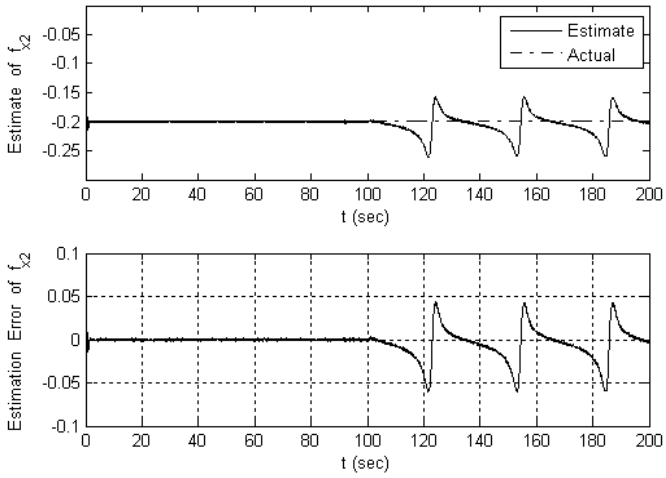

Figure 11. The actual, the estimated, and the estimation error of the fault in satellite #2 by using the reconfigurable distributed Kalman filter (RDKF) in mode *#2* (unconditional filters during the entire time interval).

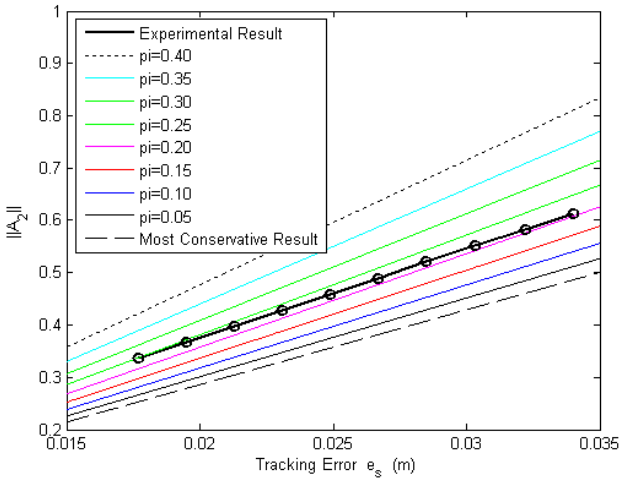

Figure 12. The analytical and simulation (experimental) values of $||A_2^T(\alpha)||$ versus the maximum allowable tracking error e_s subject to different violation probabilities π.

REFERENCES

[1] D. P. Scharf, F. Y. Hadaegh, and S. R. Ploen, "A survey of spacecraft formation flying guidance and control (Part I): Guidance", *American Control Conference*, Vol. 2, pp. 1733-1739, June 2003.

[2] D. P. Scharf, F. Y. Hadaegh, and S. R. Ploen, "A survey of spacecraft formation flying guidance and control (Part II): Control*", American Control Conference*, Vol. 4, pp. 2976-2985, 30 June-2 July 2004.

[3] S. M. Azizi and K. Khorasani, "A hierarchical architecture for cooperative fault accommodation of formation flying satellites in deep space", *IEEE American Control Conference*, St. Louis, Missouri, 10-12 June, 2009.

[4] S. M. Azizi and K. Khorasani, "A decentralized cooperative actuator fault accommodation of formation flying satellites in deep space", *IEEE Systems Conference*, pp. 230-235, 2009.

[5] S. M. Azizi and K. Khorasani, "A hybrid and switching framework for cooperative actuator fault estimation of formation flying satellites in deep space", *to appear in Asian Control Conference*, Hong Kong, August 27-29, 2009.

[6] S. M. Azizi, M. M. Tousi, and K. Khorasani, "A distributed and cooperative supervisory estimation of multi-agent systems – part I: framework", *IEEE Canadian Conference on Electrical and Computer Engineering*, St. John's, Newfoundland and Labrador, Canada, May 3-6, 2009.

[7] A. Barua, P. Sinha, and K. Khorasani, "A diagnostic tree approach for fault cause identification in the attitude control subsystem of satellites", *IEEE Transactions on Aerospace and Electronic Systems*, Vol. 45, No. 3, pp. 983-1002, 2009.

[8] Q. Cheng, P. K. Varshney, J. H. Michels, and C.M. Belcastro, "Distributed fault detection with correlated decision fusion", *IEEE Transactions on Aerospace and Electronic Systems*, Vol. 45, No. 4, pp. 1448-1465, 2009.

[9] T. E. Menke and P. S. Maybeck, "Sensor/actuator failure detection in Vista F-16 by multiple model adaptive estimation", *EEE Transactions on Aerospace and Electronic Systems*, Vol. 31, No. 4, pp. 1218-1229, 1995.

[10] N. Tudoroiu and K. Khorasani, "Satellite fault diagnosis using a bank of interacting Kalman filters", *IEEE Transactions on Aerospace and Electronic Systems*, Vol. 43, No. 4, pp. 1334-1350, 2007.

[11] P. Ferguson and J. How, "Decentralized estimation algorithms for formation flying spacecraft", *AIAA Guidance, Navigation and Control Conference*, AIAA paper number: 2003–5442, 2003.

[12] R. S. Smith and F. Y. Hadaegh, "Closed-loop dynamics of cooperative vehicle formations with parallel estimators and communication", *IEEE Transaction on Automatic Control*, Vol. 52, No. 8, August 2007.

[13] U. A. Khan and J. M. F. Moura, "Distributing the Kalman filter for large-scale systems", *IEEE Transaction on Signal Processing*, Vol. 56, No. 10, Part 1, pp. 4919-4935, October 2008.

[14] X. G. Yan and C. Edwards, "Robust decentralized actuator fault detection and estimation for large-scale systems using a sliding mode observer", *International Journal of control*, pp. 1-16, 2007.

[15] M. Basseville, "On-board component fault detection and isolation using statistical local approach", *Automatica*, Vo. 34, No. 11, pp. 1391-1415, 1998.

[16] Y. Zhang and J. Jiang, "Bibliographical review on reconfigurable fault-tolerant control systems", *Annual Reviews in Control*, Vol. 32, No. 2, pp. 229-252, 2008.

[17] Y. Zhang and J. Jin, "Fault tolerant control system design with explicit consideration of performance degradation", *IEEE Transactions on Aerospace and Electronic Systems*, Vol. 39, No. 3, pp. 838-848, 2003.

[18] Y. Zhang, "Reconfigurable control allocation against aircraft control effector failures", *IEEE International Conference on Control Applications*, pp. 1197-1202, 2007.

[19] C. Hajiyev and F. Caliskan, *Fault Diagnosis and Reconfiguration in Flight Control Systems*, Boston: Kluwer Academic, 2003.

[20] R. Kabore and H. Wang, "Design of fault diagnosis filters and fault-tolerant control for a class of nonlinear systems", IEEE Transactions on Automatic Control, Vol. 46, No. 11, pp. 1805-1810, 2002.

[21] L. Ni and C. R. Fuller, "Control reconfiguration based on hierarchical fault detection and identification for unmanned underwater vehicles", *Journal of Vibration and Control*, Vol. 9. pp. 735-748, 2003.

[22] Z. Gaoa and S. X. Ding, "Actuator fault robust estimation and fault-tolerant control for a class of nonlinear descriptor systems", *Automatica*, Vol. 43, pp. 912 – 920, 2007.

[23] J. S. H. Tsai, M. H. Lin, C. H. Zheng, S.M. Guo, L. S. Shieh, "Actuator fault detection and performance recovery with Kalman filter-based adaptive observer", *International Journal of General Systems*, Vol. 36, No. 4, pp. 375-398, 2007.

[24] W. Chen and M. Saif, "Observer-based fault diagnosis of satellite systems subject to time-varying thruster faults", *ASME*, Vol. 129, pp. 352-356, May 2007.

[25] T. Jiang, K. Khorasani, and S. Tafazoli, "Parameter estimation-based fault detection, isolation and recovery for nonlinear satellite models", *IEEE Transaction on Control Systems Technology*, Vol. 16, No. 4, pp. 799-808, July 2008.

[26] L. Xi and K. D. Kumar, "Formation control of spacecraft flying with network-induced delays and packet dropouts", *IEEE International Conference on Control and Automation*, pp. 480-485, 2010.

[27] W. Wonham, *Supervisory Control of Discrete-Event Systems*, Systems Control Group, Edward S. Rogers Sr. Dept. of Electrical and Computer Engineering, University of Toronto, Canada; available at http://www.control.utoronto.ca/DES, 2006.

[28] H. Schaub and J. L. Junkins, *Analytical Mechanics of Space Systems*, AIAA Education Series, 2003.

[29] J. Park, G. Rizzoni, and W. B. Ribbens, "On the representation of sensor faults in fault detection filters", *Automatica*, Vol. 30, No. 11, pp. 1793-1795, 1994.

[30] Y. Ru and C. N. Hadjicostis, "Fault diagnosis in discrete event systems modeled by partially observed petri nets", *Discrete Event Dynamic Systems*, Vol. 19, No. 4, pp. 551-575, 2009.

[31] D. Liberzon, *Switching in Systems and Control*, Birkhauser, Boston, MA, 2003.

[32] O. Contant, S. Lafortune, and D. Teneketzis, "Diagnosis of intermittent faults", *Discrete Event Dynamic Systems*, Vol. 14, No. 2, pp. 171-202, 2004.

[33] P. Smytha, "Hidden Markov models for fault detection in dynamic systems", *Pattern Recognition*, Vol. 27, No. 1, pp. 149-164, 1994.

[34] T. Boukhobza and F. Hamelin, "Observability analysis for structured bilinear systems: A graph-theoretic approach", *Automatica*, Vol. 43, No. 11, pp. 1968-1974, November 2007.

[35] V. Venkatasubramanian, R. Rengaswamy, K. Yin, and S. N. Kavuri, "A review of process fault detection and diagnosis part I: Quantitative model-based methods", *Elsevier Journal of Computers and Chemical Engineering*, Vol. 27, No. 3, pp. 293-311, 2003.

[36] M. W. Hofbaur and B. C. Williams, "Mode estimation of probabilistic hybrid systems", *In: HSCC 2002 (C.J. Tomlin and M.R. Greenstreet, Eds.)*, Vol. 2289 of Lecture Notes in C. S., pp. 253-266, Springer Verlag, 2002.

[37] K. Lau, S. Lichten, L. Young and B. Haines, "An innovative deep space application of GPS technology for formation flying spacecraft", *AIAA Paper96-3819*, July 1996.

[38] H.K. Khalil, *Nonlinear Systems*, Prentice-Hall, 3rd Edition, 2002.

[39] C. D. Brown, *Elements of Spacecraft Design*, AIAA Education Series, 2002.

[40] L. Ljung, *System Identification: Theory for the User*, 2nd edition. Prentice-Hall, Upper Saddle River, NJ, 1999.

[41] R. G. Brown and P. Hwang, *Introduction to Random Signals and Applied Kalman Filtering*, 3rd edition. Wiley, New York, NY, 1996.

[42] E. Semsar-Kazerooni and K. Khorasani, "Optimal consensus algorithms for cooperative team of agents subject to partial information", *Automatica*, Vol. 44, No. 11, 2008, Pages 2766-2777, 2008.